Accepted for publication in *Neuron* - Cell Press 2022

Characterization of the Critical NPAS4 Expression within an Ensemble of SOM-INs in the Primary Motor Cortex during Motor Learning

PABLO VALENTIN SERRANO

Thesis submitted to the University of Ottawa in partial fulfillment of the requirements for the Master's degree in Neuroscience

Department of Cellular and Molecular Medicine

Faculty of Medicine

University of Ottawa

ABSTRACT

GABAergic inhibitory neurons are known to play a critical regulatory role in memory formation and learning. During motor learning, pyramidal neurons (PNs) of the primary motor cortex (M1) undergo spine reorganization and firing pattern refinement. Cortical PNs are directly inhibited and regulated by two inhibitory neuronal subtypes: somatostatin-expressing interneurons (SOM-INs) and parvalbumin-expressing interneurons (PV-INs). Interestingly, SOM-mediated inhibition has been shown to regulate the observed dynamics of PNs during motor learning. Despite our expanded understanding, the molecular mechanisms that underlie these processes remain unclear. Here, I identified that the immediate-early gene transcription factor, NPAS4, is selectively expressed in a subset of SOM-INs, but not in PV-INs or PNs, during the head-fixed pellet reaching motor learning task. Furthermore, I characterized its expression pattern within the SOM-INs of M1 and found that there was no change at early phases; but as training progressed, there was a gradual increase and plateau in the number of NPAS4-expressing SOM-INs. In collaboration with other lab members, we showed that *Npas4* region- and cell-type specific deletion within SOM-INs of M1, impaired motor skill acquisition and disrupted the motor learning-induced spine reorganization. In addition, I validated and employed the novel NRAM system to examine if NPAS4 is continually expressed within the same subset of SOM-INs and found that an ensemble of SOM-INs repetitively express NPAS4 at various phases of learning. Lastly, chronic *in vivo* two-photon Ca^{2+} imaging during training showed that the ensemble of NPAS4-expressing SOM-INs had reduced activity during task-related movements compared to other SOM-

INs. Together, our results reveal an important instructive role of NPAS4 within the microcircuits of M1, in which it modulates the inhibition of a distinct subset of SOM-INs during motor learning to promote spine stabilization of downstream task-related PNs that are important for motor skill acquisition.

STUDENT'S STATEMENT

Disclaimer: This thesis contains information, figures, and data that has been accepted for publication in *Neuron* - Cell Press 2022. The research article accepted for publication is entitled "Functionally Distinct NPAS4-Expressing Somatostatin Interneuron Ensembles Critical for Motor Skill Learning". **No copyright infringement intended**. As per Cell Press embargo policies, the Journal of *Neuron* has a posting embargo period of 12 months post-publication (see appendix for links). Therefore, an embargo request of two years was submitted to the University of Ottawa upon submission of this thesis.

The entirety of project was a collaborative effort between Pablo Serrano (me), Dr. Jungwoo Yang, and Dr. Xuming Yin, under the supervision of Dr. Simon Chen. This thesis specifically highlights my contribution to the project as a first co-author, which is the characterization of the expression pattern of NPAS4 in Somatostatin-expressing interneurons during motor learning. Work conducted by Dr. Yang or Dr. Yin were explicitly stated in the text and/or supplementary figure legends.

Table of Contents

1. INTRODUCTION

1.1 Neural Basis of Learning and Memory

Learning is an important, adaptive process in an organism's life. It allows an individual to encode and store incoming information, which can be used to effectively respond to incoming stimuli based on previous experiences (1). One of the heavily focused branches of neuroscience is dissecting the processes behind learning and memory. Learning can be considered as the encoding process of memory, while memory is the learned information itself. The types of memory can be categorized into two distinct forms: declarative and non-declarative memories. Declarative or explicit memories are associated with conscious recollection of specific sematic or episodic information; while non-declarative or implicit memories are non-conscious, procedural memories that alters behavioural execution or response (2). During the learning process, memory becomes stored and consolidated in the brain to allow future recollection that could aid or modify decision-making. Identification of a specific brain region responsible for memory encoding and storage proved to be elusive. In 1920s, Lashley's 30 years of experiments attempted to uncover the brain loci responsible for memory encoding (3). Different cortical brain regions of rats were lesioned before or after exposure to various learning paradigms. However, despite various lesions, at varying degrees of disruption, memory remained preserved. Ultimately, he concluded that memory is not localized at a specific region, rather it is distributed throughout the cortex (3).

1.1A Engrams

Physical memory traces are believed to be represented by a sparse ensemble of neurons, known as engram (4). Numerous observational and experimental studies have been conducted to visualize the presence of engrams in various brain regions and to identify their role during learning and memory formation. One of the earliest studies was conducted in the amygdala, the brain region associated with emotion and fear conditioning. Transgenic labeling of activated neurons in this region during Pavlovian fear conditioning showed a significant correlation between the number of reactivated neurons and fear memory re-exposure (5). This suggested that an ensemble of neurons is repetitively activated upon exposure to a specific experience as memories become encoded and recalled. Interestingly, selective ablation of fear conditioning-activated ensemble inhibited memory formation and extinguished fear response, while ablation of a similar number of random neurons did not affect memory (6). It was then hypothesized that fear memories are stored within this neuronal ensemble during encoding, which would allow future access to stored memories during recall (4). Later, these learning-induced neuronal ensembles were referred to as engrams, and believed to represent memory traces in relevant brain regions (7).

Experience perception and behavioural response(s) during learning are multimodal. Multiple brain regions interdependently interact to encode different memory components during learning (8,9). Although most of the early engram studies were conducted in the amygdala, engram formation is not isolated within this region. Through electrophysiological recording, it has been shown that fear conditioning induces synchronization of theta waves between the amygdala and the hippocampus (8). The

hippocampus is a brain region associated with declarative memory formation. More specifically, the dentate gyrus (DG) of the hippocampus has been shown to play a critical role in contextual fear conditioning (CFC) and context discrimination. Liu et al. (2012) showed that photo-activation of CFC-engram in the DG induced a fear response without exposure to the conditioned context stimulus (10). This revealed that engrams, not only fire in response to a specific memory, but their activation can also trigger memory recall. Furthermore, this study also displays the presence of engrams at another locus, which explains how memory can be preserved despite ablation of various cortical regions. Altogether, identification and characterization of engrams present a neural construct of how memories are stored and retrieved in different brain loci.

Engrams are activated upon experience exposure and it is believed that they are formed and strengthened during learning through long term potentiation (LTP)- induced mechanisms (11,12). Experimentally, tetanic stimulation of a presynaptic neuron would activate the post-synaptic neuron that it innervates; the corresponsive activation between the two neurons would strengthen their synapses, increasing the signal transmission between the two - the premise behind LTP (13). LTP is a form of synaptic plasticity that occurs during learning, where the synaptic connections within the experience-activated neuronal ensemble are strengthened (12). The potentiated synapses would then ameliorate signal transmission allowing the neuronal ensemble to reliably fire together. Consequently, this forms an engram that stores encoded memories associated with the specific experience. As such, subsequent activation of the engram, or any neurons associated with this population, can trigger memory retrieval (4,7,14).

Altogether, these experiments elucidate various properties of the memory-encoding engrams in various brain regions. As such, engram have been characterized to have three distinct properties. First, engrams are activated during memory encoding; second, they undergo physical or chemical modifications during learning; and lastly, they are reactivated upon memory retrieval or subsequent memory presentation (12). Despite our expanded understanding of engrams in terms of their properties, role and formation, the regulatory mechanisms of their formation and/or maintenance remain unclear.

1.1B Inhibitory Engrams

To date, majority of studies on engram focused solely on excitatory neurons (14). Learning is known to induce brain plasticity in relevant brain regions through a transient decrease of inhibition, which provides a time window that permits formation of excitatory engrams to encode perceived experiences as memories (15,16). Paired stimulation of nucleus basalis with a specific tone frequency resulted in enhanced excitatory postsynaptic current (EPSC) and depressed inhibitory postsynaptic current (IPSC) in the auditory cortex. Interestingly, long-term *in vivo* cell recording of these neurons revealed that the excitatory-inhibitory (EI) balance within this cortical region was restored through a gradual recovery of IPSC, instead of excitatory cessation (15). This suggested that after the transient increase of excitation, learning also recruits ample inhibition by inhibitory neurons to restore the important cortical EI balance.

The inhibitory population consists of various subgroups, among these are two interneurons that directly inhibit and regulate the excitatory, pyramidal neurons (PNs). The somatostatin-expressing interneurons (SOM-INs) primarily sends projection to the

distal dendrites of PNs to allow regulation and fine-tuning of receptive synapses in this compartment. Meanwhile, the parvalbumin-expressing interneurons are primarily inhibit the perisomatic and somatic regions, neuronal substructure in close proximity to the axon hillock, where action potential are generated; hence PV-INs are known to effectively regulate the PNs' firing patterns (17).

As EI balance becomes restored through increased inhibition, inhibitory neurons are recruited to regulate and fine-tune synapses in PNs (17). More specifically, PV and SOM-INs have been shown to activate differentially which regulate the synapses and response of PNs (17). During fear conditioning, presentation of the aversive shock stimulus inhibited firing of both PV and SOM-INs, which disinhibited PNs and promoted synapse formation along its dendrosomatic axis (18). Meanwhile, presentation of a tone, activated PV and inhibited SOM-INs, providing a compartment-specific inhibition onto PNs (18). Interestingly, as training progressed, PV-INs became increasingly responsive to expected shock; hence, it has been hypothesized that PV-INs gate the association between the tone and the shock (19). On the other hand, SOM-INs have been shown to recruit a responsive ensemble of PNs that is specifically responsive to the fear conditioning by providing lateral inhibition across the dendrites of local PNs, which selectively regulate and fine-tune the synapses among the PN ensemble (20). Together, this demonstrates that inhibitory neurons actively regulate synaptic reorganization and ensemble formation during learning. Therefore, it has recently been hypothesized that information also becomes encoded within an ensemble of inhibitory neurons – referred as inhibitory engram (16, 18, 22).

1.2 Motor Learning and the Motor Cortex

Motor learning is an experience-dependent process that underlie motor skill acquisition and maintenance; meanwhile, a motor skill is described as a coordinated set of discrete movements performed in a continuous and overlapping sequence executed to produce an action (22). For example, a simple reach-and-grasp task encompasses gross motor movements including arm abduction and flexion during the reach, and fine motor movements as digits extend and flex during the grasp (23). Execution and refinement of this skill is what constitutes motor learning at the behavioral level. Unlike other types of learning, motor skill learning is associated with implicit, procedural memory formation; hence acquisition requires continuous and repetitive practice (22,24) This extended process of acquisition provides an opportunity to dissect the neuronal mechanism that underlies learning. In addition, the behavioural component of this process also permits quantitative measurement and analysis of learning progression.

The primary motor cortex (M1) is known to be involved in the execution of coordinated movements and regulation of voluntary movements; as such, it is also critical during motor learning (25, 26). Experimentally, it has been shown that motor learning induces increased activity in M1, while lesion studies in this area impaired motor learning both in primates and rodents (26) In addition, M1 is interconnected with various brain regions associated with motor planning, control, and adaption, a series of properties that are important during motor learning. For example, adjacent and highly interconnected with M1 are the premotor (M2) and supplementary motor areas (SMA); like M1, they also receive somatosensory, proprioceptive, and visual inputs from different brain regions. M2

and SMA have been shown to increase their activities prior to movement execution and during movement observation, implicating these regions with motor planning (27). The spinal cord also receives and sends direct or indirect projections via basal ganglia (associated with motor control and execution) to M1, which allows M1 to coordinate and control motor units, important for execution of skilled movements. Recently, it has been shown that motor learning selectively strengthens input from M1 to striatum (27), the input module of basal ganglia (29). Lastly, M1 also receives inputs from the cerebellum, associated with motor control and adaptation, through the thalamus, an important locus for relaying sensory and motor signals (27-32). Collectively, information received and relayed by M1 with other motor-associated regions constructs an optimal locus that can synergistically regulate proper movement execution and coordination, critical during motor learning.

Recently, multiple studies elucidated the dynamics of M1 neurons during motor learning. M1 is composed of a variety of neuronal subtypes that are heterogeneously distributed across multiple layers and depths. The main and most prominent type of neuron in the cortex is the excitatory PN. *In-vivo* chronic two photon Ca^{2+} imaging of layer (L) 2/3 PNs in M1 revealed a change in their firing activity patterns as mice learned a lever-press task (33). During the initial phase of training, naive movements induced highly variable activation patterns of a large population of PNs. As training progressed, the number of active PNs gradually decreased and a smaller population of movement-related stable PNs emerged. Interestingly, this refined population of neurons sequentially and spatiotemporally activate in response only to the learned movements of expert mice towards the end of training (33). Similar to excitatory engrams in other brain regions,

motor learning induces a formation of an ensemble of neurons that repetitively activates in response to formed memories - in this case, learned movements. Hence, understanding the mechanisms involved in the formation of M1 neuronal ensembles during motor learning may present new ideas as to how engrams are formed and regulated in cortical regions.

Excitatory synapses are often identified within the dendritic spines of the excitatory PNs. Therefore, synaptic plasticity is typically characterized as changes in dendritic spine density during learning. Through *in vivo* two photon spine imaging of PNs, previous studies reported that motor learning induces synaptic reorganization through formation of dendritic spines, followed by elimination and stabilization (34). Regulation is important for synaptic plasticity and the appropriate formation of neuronal ensembles. Interestingly, inhibitory inputs from SOM-INs have been shown to regulate the synaptic plasticity of PNs. Photomanipulation of SOM-INs disrupted the observed spine reorganization by dysregulating elimination and stabilization, and impaired motor learning. This suggests that SOM-INs regulate synaptic plasticity among PNs through selective synaptic pruning and maintenance (34). Furthermore, SOM-mediated regulation of PNs' synapses also affects their firing pattern at the populational level. Chemogenetic activation of SOM-INs resulted in the disruption of observed temporal shift in PNs' spatiotemporal firing during motor learning, which elucidated the role of SOM-INs in regulating PNs' activity patterns (35). Through manipulation of SOM-IN activity, both studies revealed the relationship between PNs and SOM-INs. SOM-INs' activity during motor learning actively regulates the synaptic plasticity and firing pattern of PNs, which are important neural processes that underlie learning. Although various studies have investigated the dynamics of M1 neurons

during motor learning, the molecular mechanism behind these changes remains largely unexplored.

1.3 Immediate Early Gene Transcription Factors

Neuronal activation triggers a cascade of intracellular response that induces activation of transcription factors (TFs). TFs are regulatory proteins that bind to a consensus sequence present in the promoter region(s) of downstream genes (36-37,44). Upon DNA binding, TFs recruit the RNA polymerase, forming a complex that initiates gene transcription (44). Genes regulated by TFs encode a large repertoire of proteins (and non-coding RNA) with varying functions. These downstream proteins include late-response transcription factors or effector proteins, such as enzymes, ion channel, or synaptic proteins, which can modify the intracellular physiology and connectivity of neurons (36-37,44).

Certain TFs are categorized as immediate early genes because of their fast expression upon neuronal activation (37,42). As such, they are used to identify and/or selectively manipulate activated cells during learning, including engrams (4). In the past, transgenic labeling and/or manipulation of engrams uses the promoter sequences of transcription factors such as *Fos, Arc, Npas4* and *CREB*, to drive expression of exogenous genes, including fluorophores, Cre, channelrhodopsin, tetracycline activator, etc (5-9,45-48). To identify the engrams, activated cells during learning were labelled *in vivo* using TF-driven fluorophores, and immediately after re-exposure to stimuli, (re)activated cells were labelled *ex vivo* using immunohistology (5). Colocalization of fluorophores from transgenic and immuno- labeling identified groups of repeatedly

activated neurons in response to the same experience, a key characteristic of engrams (4).

Additionally, promoters of immediate early gene TFs have also been used to drive the expression of other proteins to allow genetic or activity manipulation of the engram ensembles. For example, Guenthner et al. (2013) created a tamoxifen-dependent recombinase CreER^{T2} knock-in mouse line under the *Arc* or *Fos* promoter, this approach was called Targeted Recombination in Active Population (TRAP) (50). In TRAP mice, CreER^{T2} is expressed in an activity-dependent manner due to the utilization of *Arc* or *Fos*' regulatory elements, which confines the expression of Cre Recombinase among the active cells. However, CreER^{T2} also requires the presence of tamoxifen to bind to the estrogen receptor, which would cleave and release the membrane-bound Cre, allowing its transport to the nucleus where recombination of floxed genes occurs (51). This additional regulation of tamoxifen allows temporal control of CreER^{T2} expression to confine genetic modification within the active ensemble (controlled by regulatory element of *Fos* or *Arc*) during a particular behaviour or event (tamoxifen-regulated). Besides Cre recombinase, this strategy has also been used to drive other proteins such as tetracycline-controlled transactivator (tTA) protein. Liu et al. (2012) co-injected cFOS-tTa with TRE-ChR2-EYFP to photogenically label active ensemble (engram) in hippocampus during fear learning (10). Fos promoter will elicit the expression of tTA, allowing its binding to the tTA-response element (TRE) in the absence of doxycycline (temporal control), which will then drive the expression of channel rhodopsin and EYFP. This allowed subsequent photoactivation and labelling of neurons that were specifically active during fear learning. Interestingly, they found that photoactivation of active neurons during fear

learning was able to elicit a fear response in the absence of fear contextual cues (10). Together, these techniques demonstrate elegant utilization of TFs' activity-dependent property, which helped visualize the sparsely distributed and elusive engram that is specifically active during learning. Furthermore, these strategies has been used to delete or express specific genes, which allowed researchers to manipulate the engram and elucidate their role in memory encoding(48-50).

Apart from its activity-dependence, the regulatory role of TFs as transcription regulators/ initiators is critical for learning. Many processes that are involved in memory formation including LTP, synaptogenesis, and neuritogenesis are heavily regulated by the expression of synaptic proteins induced by TFs (43,49). For example, when CREB was selectively repressed in engram-forming neurons of the DG during CFC, learning was impaired. This was partly due to the downregulated expression of CREB's downstream gene, Atf3, involved in actin structural plasticity (48). This study describes a detrimental role of TFs in regulating protein expression and neuronal processes. Additionally, it highlights the importance of TFs as a molecular component that links neuronal activation, synaptic plasticity, and engram formation together, which are the series of processes that typically occurs during learning.

1.3 A Neuronal PAS 4 (Npas4)

Over the years, many TFs have been identified to play an essential role in learning (40,43,52), and one of these TFs is the activity-dependent, immediate early-gene, Neuronal PAS Domain 4 (Npas4). Ramamoorthi et al. (2011) showed that NPAS4 is highly and critically expressed in CA3 hippocampus during CFC. In addition, they found

that region-specific *Npas4* knock out in CA3 resulted in impaired long-term memory formation, and re-introduction the TF by viral infection rescued learning (40). Recently, it has also been reported that NPAS4 is involved in learning-related synaptic plasticity and engram formation (47). CFC-induced NPAS4 expression in CA3 selectively strengthens synaptic inputs from the mossy fibers, revealing the NPAS4's regulatory role in selective potentiation of signal transmission from specific neural inputs during learning (47). Interestingly, it has also been shown that NPAS4 forms a genetically distinct neuronal ensemble within the engram population that is genetically distinct from another ensemble, delineated by their expression of FOS (45). Through the use of the novel NPAS4-driven Robust Activity Marking (NRAM) system, it was demonstrated that a specific NPAS4-forming ensemble, is formed in the DG during CFC to selectively recruit input from cholecystokinin-expressing interneurons (CCK-INs) (45). Similar to other engram-labelling strategies, NRAM uses an NPAS4-binding promoter to drive the expression of a fluorophore in a doxycycline-dependent manner (45,46). This approach was used to label and electrophysiologically record from NPAS4-expressing cells in DG during CFC, which revealed that the NPAS4-expressing ensemble selectively recruits IPSC from CCK-INs, promoting memory discrimination (45). Together, these studies identify synaptic plasticity and engram formation as the learning-induced mechanisms related to NPAS4 expression in CA3 and DG hippocampus during CFC. Furthermore, they showed that engrams can be genetically heterogenous based on their expression of different transcription factors, such as NPAS4 and/or FOS. Despite our expanded understanding of NPAS4's role in learning, majority of these studies were conducted in the highly organized structure of the hippocampus during CFC, an explicit type of learning. It remains unclear whether NPAS4

regulates learning-related processes within the cortical regions during an implicit type of learning, such as motor skill acquisition.

Previous NPAS4 cortical studies mainly dissected its expression pattern in the visual cortex upon sensory experience. NPAS4 has been shown to be uniquely expressed both in excitatory and inhibitory cortical neurons in the visual cortex (42). Spiegel et al. (2014) demonstrated that when dark-housed mice were exposed to light, both excitatory and inhibitory neurons of the visual cortex expressed NPAS4. Interestingly, NPAS4 induces distinct transcription profiles in each neuronal subtype, suggesting that it regulates specific downstream genes depending on the cell-type (42). More specifically, NPAS4 upregulates the expression of proteins affecting either EPSC or IPSC depending on the cell-type (38,39). Therefore, it has been suggested that NPAS4 plays a modulatory role in facilitating the homeostatic balance and remodelling of excitation and inhibition within the cortical neural circuitry, which is also critical during learning (42).

In my thesis, I aim to investigate the expression pattern of NPAS4 during motor learning to further elucidate how NPAS4 facilitates learning-related mechanisms in M1. Using immunofluorescent staining of NPAS4 and transgenic labelling of different neuronal cell-types, I investigated the expression pattern of NPAS4 across different neuronal populations in M1 at various phases of motor learning. Furthermore, I validated the properties of a newly-developed NPAS4-dependent robust activity marking system and used this technique to label NPAS4-expressing cells in vivo to elucidate the re-expression pattern of NPAS4 in SOM-INs at two different time points during motor learning.

1.4 Research Statement

We employed an automated head-fixed pellet-reaching task as a motor learning paradigm that would allow quantification of motor skill acquisition, specifically by the left forepaw, while minimizing compounding variables from other non-learning-related movements. Using this paradigm, we dissected the expression pattern of NPAS4 in M1 during motor learning and found that NPAS4 is highly expressed in M1 of trained mice compared to non-trained controls. Interestingly, NPAS4 ’s expression is selectively up-regulated within the SOM-IN population of M1, and not in PV-INs or PNs, suggesting a cell-type specific expression of this TF during motor learning. Using a newly developed NPAS4-driven Robust Activity Marking (NRAM) system, I identified an engram-forming subpopulation of SOM-INs that repetitively express NPAS4 at various phases of learning. In collaboration with other lab members, we validated the importance of cell-type specific expression of NPAS4 in SOM-INs of M1 during motor learning. We found that NPAS4 expression in SOM-INs regulates synaptic reorganization by reducing the activity of NPAS4-expressing SOM-INs. Altogether, my thesis elucidates the cell-type specific expression pattern of NPAS4 and presents a potential molecular link behind the underlying mechanisms of SOM-mediated regulation throughout motor learning.

2. AIMS & HYPOTHESIS

1. Investigating the expression pattern of NPAS4 during motor learning requires establishment of a motor learning paradigm that would allow quantification of the rate of learning. Therefore, we employed the head-fixed pellet reaching task as a motor learning paradigm, which allowed us to quantify the motor learning rate based on the number of successful trials.

2. After the establishment of a motor learning paradigm, we next aimed to determine if NPAS4 is expressed and is important in M1 during motor learning, using immunofluorescent staining and local conditional knockout of *Npas4* in M1, respectively.

> We hypothesized that if NPAS4 plays an important role in M1 during motor learning, then its expression level should change from baseline after training, and its deletion should affect motor skill acquisition.

3. We observed that motor learning induced a critical increase of NPAS4 expression in M1. Next, we aimed to identify the cell-type specific expression pattern of NPS4 among different cell-types in M1 during motor learning. Therefore, we subjected different mouselines with transgenically-labelled PNs, SOM- or PV- INs to the head-fixed pellet reaching task and immunostained for NPAS4.

> If NPAS4 is selectively expressed in a specific cell-type during motor learning, then we should observe an increased colocalization between the transgenically-labelled subtype and NPAS4 staining after training. Furthermore, its cell-type specific deletion should also affect motor skill acquisition.

4. We observed that NPAS4 is selectively and critically expressed in SOM-INs of M1 during motor learning. Next, we aimed to determine if NPAS4 is re-expressed in the same ensemble of SOM-INs at various time points during motor learning; hence, we employed the newly-developed NPAS4-driven Robust Activity Marking (NRAM) System to label NPAS4-expressing cells *in vivo*. Prior to its utilization, we first aimed to validate its activity- and NPAS4- dependent properties, its doxycycline-regulated Tet-off system, and its ability to effectively label NPAS4-expressing cells during motor learning.

5. After validating the effectivity of the NRAM system, we employed this strategy to characterize the expression pattern of NPAS4 within SOM-INs at early (T3) and late phases (T7 or T12) of learning.

If motor learning induces a formation of NPAS4-expressing SOM-IN ensemble, then NPAS4 must be re-expressed in a subgroup of SOM-INs at multiple timepoints during motor learning.

3. RESULTS

3.1 Establishing an Automated Head-fixed Pellet Reaching Task as a Motor Learning Paradigm

To investigate the NPAS4's expression pattern in M1 during motor learning, we first established the head-fixed pellet reaching task, adapted from the classic freely moving pellet reaching task (23). Head-fixation minimizes confounding variables from regular movements associated with the freely moving paradigm as it specifically allows neuronal activation from the reach-and-grasp movements related with the task. In addition, it permits effective in vivo imaging of M1 neurons under two-photon microscopy as mice perform the task. In this task, food restricted mice were trained to use their left hand, regardless of hand preference, to reach and grab a food pellet from an automated motorized bar, every 30 seconds (1 trial). Mice underwent 12 consecutive sessions: 1 session/ day with 60 trials/ session (Figure 1A-B). Mice subjected to training quickly learned to reach for the pellet, and their successful rates gradually improved over sessions. Quantitative behavioural analyses showed a significant and gradual increase of success rate, followed by a plateau from T7 to T12 (Figure 1C). These demonstrate that the head-fixed pellet reaching task presents a learning curve consistent with other motor learning paradigms (23,24), hence we used this paradigm to investigate the expression pattern and role of NPAS4 during motor learning.

3.2 Increased NPAS4 Expression is Important during Motor Learning

3.2A Motor Learning Increased NPAS4 Expression in M1

NPAS4 is an activity-dependent TF that fine tunes the excitatory-inhibitory balance within the neural circuitry, which is important for learning (38,39,42). Meanwhile, motor learning induces synaptic reorganization among inhibitory and excitatory neurons in M1 (34). Hence, we hypothesized that NPAS4 serves as a key regulator in mediating the excitatory-inhibitory reorganizations in M1 that are crucial for motor learning. To investigate this, I first perfused and sliced brain samples collected from non-trained (NT) mice and mice that underwent 12 days of training (T12). As mentioned, mice were specifically trained to use their left paw (regardless of paw preference); hence, I performed immunofluorescent staining on brain slices containing the right contralateral hemisphere of M1 to examine NPAS4 expression (Figure 2A-B). I found a significant increase in NPAS4-expressing ($NPAS4^+$) cells in T12 mice compared to the NT controls (NT = 20.6 ± 8.23 cells/mm^2; T12 = 88.9 ± 7.62 cells/mm^2; Figure 2C). This demonstrates that NPAS4 expression is upregulated in M1, which hints to a potential role in motor learning.

3.2B Regional *Npas4* in M1 Knock Out Impaired Motor Learning

In collaboration with another lab member (Dr. Jungwoo Yang), we ascertained the importance of NPAS4 expression in M1 during motor learning. For this, we utilized a cre-dependent *Npas4* conditional knockout mouse line ($Npas4^{flx/flx}$) and unilaterally injected AAV-Cre into the contralateral M1 to regionally delete *Npas4* in $Npas4^{flx/flx}$ mice (Npas4 cKO). For control, $Npas4^{flx/flx}$ mice were injected with AAV-GFP instead of AAV-Cre

(Supplementary Figure 1A). After 3 weeks of recovery, Npas4 cKO and control mice were subjected to the head-fixed pellet reaching task. We found that Npas4 cKO mice failed to learn the task with no improvement in success rate. In contrast, control mice showed the typical improvement of success rate (Supplementary Figure 1B). Noticeably, the attempt rate and grip strength were comparable between the two groups (Supplementary Figure 1C-D), suggesting that *Npas4* deletion did not affect the animals' digit strength, arm movement, or the ability to associate hand-movement with food rewards. Together, this suggests that increased NPAS4 expression in M1 is critical during motor learning.

3.3 Selective Expression of NPAS4 within SOM-INs of M1 is Critical during Motor learning

3.3A NPAS4 is Selectively Expressed within SOM-INs during Motor Learning

NPAS4 expression has been observed both within excitatory and inhibitory neurons (42). In M1, the most well-studied neuronal subtypes that are involved in motor learning are the excitatory pyramidal neurons (PNs) and the inhibitory, dendrite-targeting somatostain-expressing interneurons (SOM-INs) and soma-targeting parvalbumin-expressing interneurons (PV-INs) (Figure 3A). Therefore, I next investigated the cell-type specific expression of NPAS4 within these neuronal subtype populations of M1 during motor learning. To transgenically label each cell type, we independently crossed *EMX-cre* (expresses cre in PNs), *SOM-cre*, or *PV-cre* mice with a cre-dependent tdTomato reporter mouse line (*Ai14*). Subsequently, the newly generated mouse lines were subjected 12 days of training and immunofluorescently stained for NPAS4 (Figure 3B).

Surprisingly, I observed no significant increase of NPAS4$^+$ PNs, and minimal increase of NPAS4$^+$ PV-IN in T12 mice compared to NT control of each respective mouse line (Figure 3C-D). In contrast, the number of NPAS4$^+$ SOM-IN at T12 showed a significant increase compared to NT control (Figure 3E). To determine if NPAS4 was also minimally expressed in PNs and PV-INs at the beginning of learning, I stained for NPAS4 expression at T1 and T3 and found that there was still no increase in NPAS4 expression in each cell-type at early phases of training relative to NT controls (Figure 3F-G).

Since NPAS4 was specifically expressed within the SOM-IN population, I characterized the time course of NPAS4 expression within the SOM-IN population of M1 at various phases of learning. By training and collecting the brain samples of *SOM-cre::Ai14* mice at different time points (shaping, T1, T3, T7, and T10), I observed a gradual increase of NPAS4$^+$ SOM-INs until T7, which then plateaued until T12 (Figure 3H-I). Noticeably, seizure induction with kainic acid showed maximal NPAS4 expression across M1 (Figure 3J). Interestingly, only ~10% are SOM-INs which suggests that NPAS4 is expressible in all cell types, demonstrating that NPAS4 is not only intrinsically expressed in the SOM-IN population of M1. Together, this suggests that motor learning induces a cell-type specific expression of NPAS4 within the SOM-INs of M1. SOM-INs have been shown to specifically regulate dendritic spine elimination and stabilization of PNs, which occurs at later phases of motor learning (34). Therefore, the selective and late expression of NPAS4 in SOM-INs during the head-fixed pellet reaching task, hints to a potential role that this TF plays in regulating spine dynamics during motor learning, particularly synaptic pruning and maintenance.

3.3B Regional and Cell-type Specific Knock Out of *Npas4* within SOM-INs of M1 Impaired Motor Learning

To investigate if SOM-specific expression of NPAS4 is important during motor learning, we selectively deleted *Npas4* in PN, SOM-INs, or PV-INs of M1. For this, Dr. Jungwoo Yang employed the CRISPR-Cas9 strategy, combined with the Cre-recombinase system by crossing *EMX-cre, SOM-cre,* or *PV-cre* mouse lines with *ROSA-LSL-Cas9-GFP* mice to selectively express Cas9 in each cell type. Next, *Npas4*-targeting sgRNA ($sgRNA^{Npas4}$) were injected into the right M1 of *EMX-cre::Cas9, SOM-cre::Cas9*, and *PV-cre::Cas9* mice to regionally KO *Npas4* in PNs, SOM-INs, and PV-INs, respectively (Supplementary Figure 2A). Meanwhile, control mice from each mouse line were injected with LacZ-targeting sgRNA. Three weeks after surgery, mice were subjected to the motor learning paradigm. Interestingly, we observed comparable success rates across training days between the control, *Npas4* PN KO, and *Npas4* PV-IN KO mice. In contrast, *Npas4* SOM-IN KO mice exhibited a significant reduction in success rate compared to the control without showing differences in attempt rate and grip strength (Supplementary Figure 2 B-D). Together, this demonstrates that selective deletion of *Npas4* within SOM-INs, and not PN or PV-INs in M1, impairs motor learning. These results demonstrate the important role of NPAS4 during motor learning through its selective expression within SOM-INs.

3.3C Majority of NPAS4^{+} SOM-INs during Head-fixed Pellet Reaching Task are Martinotti SOM-INs

Recent work has further categorized SOM-INs into 2 broad groups: Martinotti and non-Martinotti SOM-INs (53). Martinotti SOM-INs have previously been characterized by their expression of calbindin (CalB) and calretinin (CR) proteins (53,54). Since no one has characterized Martinotti SOM-INs in M1 before, I first aimed to validate the presence and quantify the number of Martinotti SOM-INs in M1. Using *SOM-cre::Ai14* brain samples containing NPAS4-labeled cells at T12 (NPAS4^{+} cells were labelled *in vivo*, using an NPAS4-dependent robust activity marking system) and immunostained them for CalB and CR (Figure 4 A-D). Interestingly, I found that ~45% of M1 SOM-INs were Martinotti cells (CalB+ SOM-INs = 34.3 ± 3.7%, CR+ SOM-INs = 11.0 ± 2.4%, Overlap = 6.3 ± 1.2 %; Figure 4E), which is similar to previous observations in the somatosensory cortex (53). Furthermore, among the T12 NRAM-expressing SOM-INs, ~70% were identified as Martinotti SOM-INs (CalB^{+}NRAM^{+}SOM-INs = 42.6 ± 7.6%, CR^{+}Npas4^{+}SOM-INs = 27.8 ± 5.0 %; Figure 4F). Previous study showed that learning-induced spine reorganizations during motor learning occurs in the distal dendrites of PNs. Since Martinotti SOM-INs are known to specifically project and arborize at L1 (53,55), our observation supports the idea that NPAS4 expression within SOM-INs regulates the spine reorganization on distal dendrites of PNs during motor learning (Supplementary Figure 4). Overall, these findings demonstrate that the selective expression of NPAS4 within a specific subtype of SOM-INs during motor learning regulate previously described domain-specific spine changes in PNs (34).

3.4 NPAS4 is Repetitively Expressed within an ensemble of SOM-INs during Head-fixed Pellet Reaching Task

3.4A Validating the NPAS4-driven Robust Activity Marking (NRAM) System

Re-expression of learning-related TF's have previously been observed in the formation of engrams, an important process in memory encoding (4-7,9). Since motor learning induced elevated levels of NPAS4 expression within the SOM-IN population as early as T3, this raised an interesting question if NPAS4 is also re-expressed in an engram of SOM-INs to encode memory. Expression of NPAS4 is transient and degrades quickly after induction (38,40); to label NPAS4$^+$ cells at 2 different timepoints, Dr. Yingxi Lin's lab at SUNY developed a strategy to label NPAS4$^+$ cells *in vivo*, named NPAS4-driven robust activity marking (NRAM) system (45). NRAM's promoter is a consensus sequence and a binding site for NPAS4, which would drive the expression of a fluorescent protein (GFP or mKate2). Moreover, it is regulated by a doxycycline (DOX)-dependent Tet-off system that can temporally control the labeling of NPAS4$^+$ cells (Figure 5A). To validate its properties, I injected AAV-NRAM-mKate2 (or GFP) in the M1 of mice and induced seizure with or without the presence of DOX in their liquid diet. The two viruses labelling NPAS4-expressing cell in GFP or mKate2 were both tested because we planned to use the NRAM system in transgenically-labelled SOM-INs::Ai14 mice (red); or combine it with Ca^{2+} imaging using GCaMP (green). I found low density of NRAM-positive (NRAM$^+$) cells in home-caged mice that were not under DOX liquid diet (Figure 5 B-D). When I induced seizure in another cohort of mice, high expression of NRAM$^+$ cells were observed in the absence of DOX, whereas mice under DOX liquid diet maintained low expression

of NRAM$^+$ cells (Figure 5B-D). This confirms the NRAM system's activity-dependent and DOX-regulated neuronal labeling properties. Since NPAS4 degrades faster than the expression of NRAM-driven fluorescent proteins (Figure 5B, E-F), I also validated the NPAS4-dependent property of NRAM by injecting sgRNA^{Npas4} and AAV-NRAM-mKate2 in *EMX-cre::Cas9-GFP* mice to selectively delete *Npas4* in PNs. I then induced seizure to maximally activate NRAM in the brain. The controls were *EMX-cre::Cas9-GFP* mice injected with AAV-NRMA-mKate2 only (Figure 5G). As a result, I found significantly reduced NRAM$^+$ cells among the GFP-expressing PNs in *Npas4* PN KO mice compared to control ones, demonstrating the NPAS4-dependent property of the NRAM system (Figure 5H-I). Lastly, I validated if NRAM can also label NPAS4$^+$ cells in similar levels as immunofluorescent staining during motor learning. Previous studies demonstrated that the removal of DOX 48 hours prior to behavioural studies optimized NRAM *in vivo* labeling (45). We wanted to use the NRAM system to label NPAS4-expressing cells *in vivo* during early phase of learning; since I observed a significant increase in NPAS4$^+$ SOM-INs as early as T3 (Figure 3I), I injected *SOM-cre::Ai14* mice with AAV-NRAM-GFP and subjected them to training after 3 weeks of recovery and DOX was removed for 48 hours, subsequently after T1, to label NPAS4$^+$ cells at T3. I found significant high density of NRAM$^+$ SOM-INs at T3 compared to the home-caged control mice that had DOX liquid removed for 3 days. Furthermore, the percentage of NRAM$^+$ SOM-INs at T3 was similar compared to the immunofluorescently stained NPAS4-expressing SOM-INs (Figure 4J-L). Together, this shows that the NRAM system can effectively label NPAS4-expressing cells *in vivo* in activity- and DOX- dependent manners during motor learning.

3.4B NPAS4 is Persistently Expressed in an Ensemble of SOM-INs from Early to Late Phases of Learning

SOM-INs have been shown to regulate the spine reorganization of PN's distal dendrites during motor learning. During this process, SOM-mediated spine elimination and stabilization were observable between T4 and T7, respectively (34). Interestingly, we observed a significant increase in NPAS4$^+$ SOM-INs as early as T3, followed by a plateau beginning at T7. If the same ensemble of SOM-INs is regulating spine reorganization across training days, and NPAS4 plays a role in this process, one would hypothesize that NPAS4 must also be re-expressed within of the same ensemble of SOM-INs. To examine if NPAS4 is re-expressed in an ensemble of SOM-INs at different timepoints of learning, we injected AAV-NRAM-GFP in the M1 of *SOM-cre::Ai14* mice and removed DOX from T1 to T3 to label NPAS4$^+$ cells at T3 (early phase). Mice were then continuously trained until T7 or T12 and immunofluorescently stained to label NPAS4$^+$ cells at each respective time point (late phases) (Figure 6 A-B). Co-localization between T3 NRAM$^+$ SOM-INs and T7 or T12 NPAS4$^+$ SOM-INs will reveal how much of the population continuously expressed NPAS4 both at the early and late phases of learning (Figure 6 C-D). Interestingly, we observed that 44 ± 5% of T3 NRAM$^+$ SOM-INs re-expressed NPAS4 at T7, and 18 ± 6% re-expressed the TF from T3 to T12 (Figure 6E). In addition, we compared the co-localization of non-task specific NRAM$^+$ SOM-INs (DOX off for 48 hours in home cage) to T3 NRAM$^+$ SOM-INs. We observed that the percentage of colocalization between NT labelled NRAM$^+$ SOM-INs and T12 NPAS4$^+$ SOM-INs were significantly lower than T3 NRAM$^+$ SOM-INs (Figure 6F), which suggests that a functionally significant ensemble of SOM-INs already re-expressed NPAS4 at T12, as early as T3. Together,

this demonstrates that a small population of NPAS4-expressing SOM-INs, recruited at the early phase of learning, continuously reactivate and re-express NPAS4 until the later phases. These results hint to a potential mechanism on how NPAS4 regulates synaptic plasticity during motor learning – through its continuous expression within an ensemble of SOM-INs.

4. DISCUSSION

4.1 Summary

In this thesis, I report the selective expression of NPAS4 within the SOM-INs of M1 and describe its expression pattern in SOM-INs at different phases of learning. Using the automated head-fixed pellet reaching task as a motor learning paradigm, I found that motor skill acquisition induces increased NPAS4 expression in M1. Interestingly, learning-induced NPAS4 upregulation was primarily within the SOM-IN population, and not PV-IN or PNs. More specifically, I found that ~70% of L2/3 and L5 NPAS4$^+$ SOM-INs were Martinotti cells, which are known to innervate L1. Meanwhile, work in our lab also found that region- and cell-type specific deletion of *Npas4* in SOM-INs of M1 is critical for motor learning. To characterize the expression pattern of NPAS4$^+$ SOM-INs at different stages of learning, I trained six cohorts of *SOM-cre::Ai14* mice, perfused each cohort at different time points during training (shaping, T1, T3, T7, T10, or T12), and immunostained the brain slices for NPAS4. I found that NPAS4$^+$ SOM-INs did not change at shaping and T1 compared to non-trained animals. Interestingly, the number of NPAS4$^+$ SOM-INs gradually increased from T3 until T7 and plateaued until T12. Lastly, I validated and employed the novel NRAM system to examine if NPAS4 is continually expressed within the same subset of SOM-INs during various phases of learning. By comparing the colocalization between NRAM labelled cells at T3, and immunostained NPAS4$^+$ cells at T7 or T12, we found that an ensemble of SOM-INs re-expresses NPAS4 at different phases of motor learning. Altogether, this study elucidates the critically selective expression of NPAS4 in SOM-INs of M1 during motor learning; and characterizes its

expression pattern within the SOM-IN population at various timepoints throughout motor learning.

4.2 Implications of cell-type specific expression of NPAS4 within SOM-INs and the formation of NPAS4-expressing SOM-IN ensemble during motor learning

How does NPAS4 expression within SOM-INs regulate motor learning? Work from my lab mate combined in vivo two-photon Ca^{2+} imaging of SOM-INs and NRAM labelling cells at T3 and investigated this question at the neuronal population level. In general, we found an increase activity in all SOM-INs during reach-and-grasp (RB) bouts. However, after categorizing SOM-INs into $NRAM^{+}$ or NRAM-negative ($NRAM^{-}$), we revealed that $NRAM^{+}$ SOM-INs at T4 had significantly reduced firing pattern compared to other SOM-INs during task-related movements (Supplementary Figure 3). Previous work by Adler et al. (2019) also described an ensemble of SOM-INs that showed reduced activity during a treadmill motor learning task and demonstrated that these SOM-INs specifically regulate PNs' spatiotemporal firing patterns during learned movements (35). Combined with our observations (Supplementary Figure 3), it is likely that the population of SOM-INs with lower activity, delineated by their expression of NPAS4, also share the same function as the SOM-INs (reduced firing) described in Adler's study. This hypothesis presents a potential mechanism on how NPAS4 expression within an ensemble of inhibitory SOM-INs regulate and refine excitation from PNs, which recapitulates the importance of excitatory-inhibitory regulation at the populational level during learning.

At the subcellular level, motor learning induces dendritic spine reorganization of the distal dendrites of PNs, which is characterized by increased spine formation, followed by elimination, and stabilization. Interestingly, inhibition from SOM-INs, but not PV-INs, has been shown to regulate the elimination and stabilization of these dendritic spines during motor learning. Therefore, the observed selective and critical expression of NPAS4 within SOM-INs suggests a potential role that NPAS4 plays in regulating learning-induced synaptic plasticity during motor learning. This is supported by another experiment in the lab demonstrating that *Npas4* SOM KO in M1 impaired spine elimination during motor learning (Supplementary Figure 4). Together with the observed preferential expression of NPAS4 in Martinotti SOM-INs (Figure 4) and the attenuated success rate of *Npas4* SOM KO mice (Supplementary Figure 2), we demonstrate that NPAS4 actively regulates the spine reorganization at the distal dendrites PNs' through its selective expression within the inhibitory SOM-IN population - an important process of motor learning.

The level of inhibition is an important regulatory mechanism for synaptic potentiation and depression, which determines spine stabilization or elimination, respectively (34,56-58). Ca^{2+} imaging revealed an ensemble of $NRAM^{+}$ SOM-INs with reduced activity (Supplementary Figure 3), which suggests that NPAS4 expression reduces SOM-IN activity. When SOM-IN is inhibited via NPAS4 expression, the release of GABA onto PNs is reduced, which allows potentiation of the dendritic spines innervated by the $NPAS4^{+}$ SOM-INs; therefore, we postulate that the $NPAS4^{+}$ SOM-IN ensemble is disinhibited to promote stabilization of task-related dendritic spines. Overall, NPAS4's expression within a specific ensemble of SOM-INs can explain how selective elimination and stabilization are regulated at the molecular level. It portrays how the described

regulatory role of SOM-INs can be modulated within the neural circuitry to allow selective elimination and stabilization of dendritic spines during synaptic plasticity, which is an important process of motor learning.

The observed NPAS4 re-expression within an ensemble of SOM-INs suggests the formation of an NPAS4-forming inhibitory engram during motor learning. As mentioned, inhibitory engrams are also believed to store information from learning that is specific to a particular experience or memory (16,18). Therefore, we hypothesize that motor learning establishes a task-specific NPAS4-expressing SOM-IN engram, where similar tasks would form NPAS4-expressing ensembles with greater overlap, than the ensembles formed during different tasks. Formation of a task-dependent SOM-IN engram would induce modification and stabilization of synapses at the dendritic branches of downstream PNs in a task-dependent manner. Interestingly, Yang et al (2014) showed that memory consolidation of a motor skill induces a branch-specific Ca^{2+} activity in PNs, a process that is dependent on SOM-IN regulation. They showed that forward running induces spine dynamics in one branch, while forward and backward running would elicit spine dynamics at two separate dendritic branches (59). Since different ensembles of SOM-INs likely send more projection to one dendritic branch over another, this would allow the branch-specific spine dynamics of PNs during forward and backward running. Therefore, NPAS4 expression in a select ensemble of SOM-INs could explain the described differential regulation among different PNs' dendritic branches. Overall, the distinct expression pattern of NPAS4 within an ensemble of SOM-INs presents a potential molecular mechanism of inhibitory engram are formed, and describes how task-dependent changes in PNs are regulated during motor learning.

4.3 Future Directions

Neurons recruited to form an engram during learning typically receive inputs from relevant brain region(s). NPAS4 engram-forming cells in the CA3 hippocampus have been shown to receive enhanced presynaptic connections from the DG, via mossy fibers during CFC (45). Future work will involve identifying and characterizing the inputs received from the described motor learning-induced NPAS4$^+$ SOM-IN engram in M1. We found that ~70% of NPAS4$^+$ SOM-INs during the head-fixed pellet reaching task were Martinotti cells, which primarily project to L1 dendrites of PNs. Interestingly, cortical SOM-INs, particularly Martinotti cells, receive inputs both locally and distantly from other brain regions. Cortical SOM-INs are known to receive local disinhibitory inputs from VIP-INs, which regulates its inhibition and activity pattern (60). Meanwhile, cortical Martinotti cells have been shown to also receive input from distal regions, recruited specifically for gradual lateral inhibition (61,62). Characterization the inputs received by NPAS4$^+$ SOM-INs during motor learning, will expand our understanding of the regulatory role of SOM-INs in the M1, particularly Martinotti SOM-INs. In addition, it may reveal how genetically distinct inhibitory engrams are formed and further elucidate their functional role within the cortical circuitry during learning.

NPAS4's expression can be modulated and/or downregulated depending on the presence of other proteins (41,63,64). It has been shown that the presence of Histone Deacetylase 5 (HDAC5) binds to the enhancer region of Npas4 and downregulates its transcription (63). Meanwhile, different isoforms of ARNT dimerizes with NPAS4, where distinct downstream genes are regulated depending on which heterodimers are formed (41,64). It would be interesting to identify the proteins co-expressed with NPAS4 during

motor learning to determine how NPAS4 is regulated and how it regulates various downstream genes. Identification of proteins that downregulate NPAS4 expression, such as HDAC5, may present a potential mechanism of how NPAS4 is selectively expressed within SOM-INs during motor learning. In addition, elucidating the dimerization and regulatory pattern of NPAS4 as a TF may reveal the genes associated with the observed reduced firing of $NRAM^+$ SOM-INs, and further characterize how $NPAS4^+$ SOM-INs regulate synaptic plasticity and neuronal EI balance, at the molecular level, during motor learning.

5. METHODS

Animals

All experimental work with the animals were in accordance to the protocols approved by the University of Ottawa Animal Care Committee and Canadian Council on Animal Care guidelines. Mouse lines used in the experiments: WT (*B6129SF1/J*; Jackson Laboratory, Stock No. 101043), *Npas4*$^{flx/flx}$ (from Dr. Michael E. Greenberg, Harvard University), *Rosa26-LSL-Cas9* (Jackson Laboratory, Stock No. 026556), *SOM-IRES-Cre* (Jackson Laboratory, Stock No. 013044), *PV-IRES-Cre* (Jackson Laboratory, Stock No. 008069), *Emx1-IRES-Cre* (Jackson Laboratory, Stock No. 005628), Ai14 (Jackson Laboratory, Stock No. 007914). *SOM-IRES-Cre::Ai14, PV-IRES-Cre::Ai14*, or *Emx1-IRES-Cre::Ai14* mice were generated by crossing *Ai14* males with *SOM-IRES-Cre, PV-IRES-Cre* or *Emx1-IRES-Cre* females, respectively. *SOM-IRES-Cre::Rosa26-LSL-Cas9, PV-IRES-Cre::Rosa26-LSL-Cas9* or *Emx1-Cre::Rosa26-LSL-Cas9* were generated by crossing *Rosa26-LSL-Cas9* males with *SOM-IRES-Cre, PV-IRES-Cre* or *Emx1-IRES-Cre* females, respectively. All colonies were bred in a housing room facility with 21-23 ^{o}C temperature and 40-60% humidity. Experimental mice were housed in ventilated plastic cages in a reversed light cycle (12h/12h) room. Male and female mice between age 8 – 14 weeks were used for experiments. Unless specified, controls were littermates with the same genetic background.

Automated head fixed pellet reaching task

Adapted from freely moving pellet-reaching task (23). Two to three days prior to training, baseline weights of mice were measured, and mice were placed under food-restriction. Food-restricted mice were regularly weighed and given 1.5-2.0 g of food chow/day to maintain their weights at ~85% of their baseline. Next, mice underwent 2 days of habituation, pretraining and 12 days of training. Habituation: head-fixed in the training chamber for 15-20 minutes and given food pellets in the home cage. Head-fixation: apparatus clipped the head bar metal implant (see Methods – Surgery) to restrain head movements; to keep the body straight relative to the head, the mice's lower forelimbs were kept in a plastic tube. Pretraining: head-fixed mice were provided food pellets using a tweezer; to instigate left arm movements, pellets were given slightly to the left side of the mice. Once mice autonomously reach at least 3 times in response to the automated pellet holder, animals allowed to progress to the training stage. Training: food pellet was presented slightly below, at the left side of the mice's head (12 mm below and 8 mm to the left of the nose) by an automated pellet holder. A trial consisted of the motor arm up for 30 seconds, followed by a 5 seconds intertrial interval (ITI; motor arm down). Each session consisted of 60 trials, 1 session/day for 12 days. Behavioral performances were assessed through post-analysis of recorded videos. Mice behaviour were categorized into 3 types: 'Success', 'Miss', or 'No attempt'. Success: mouse reaches and grabs the pellet using its left paw and places the food in its mouth. Miss: any attempt made by the left hand that did not result in a success. No attempt: right paw was used or no movement towards the food were made. 'Success' and 'No Attempt' rates were calculated as ratios: 'Success' or 'No Attempt' trials / 'Success' + 'Miss' + 'No Attempt'. Trials where the

automated holder failed bring up a food pellet were not considered. Experimenters were blinded in the manipulated conditions.

Surgery for head fixed pellet reaching task and viral vector delivery

Mice were injected subcutaneously with buprenorphine (0.05 mg/kg), Baytril (5 mg/kg), and Dexthamethasone (2 mg/kg) for analgesia, anti-infection, and anti-inflammation, respectively. Constant flow of 1-2% of Isoflurane was used to induce and maintain the mice in an anesthetized state. Circular incision was made to remove the scalp and expose the skull. Skull was scraped using scalpel blade to remove connective tissues and increase skull's surface area. A customized metal head plate or bar was glued onto the skull (Krazy Glue). A circular skull opening (Diameter: ~2 mm) was created above the right motor cortex. Virus vectors were slowly injected in the M1 to prevent backflow (see below for details regarding the virus and mouse lines). After virus injections, a glass window was placed on top of the M1 for mice that underwent two-photon microscopy. Implants were stabilized and skull opening was covered with Jet Denture Repair Powder Cement (Henry Schein). Mice were allowed to recover in home cage for ~2-3 weeks before behavioral training.

***Npas4* regional M1 cKO:** M1 of *Npas4*$^{flx/flx}$ mice were injected AAV1-CMV-PI-Cre at 250 µm and 500 µm depth (250 nl /site) from pia. Control group was injected with the AAV-Flpo and AAV-Flp-GFP mixture viruses without the AAV-Cre.

***Npas4* cell-type specific and regional M1 cKO:** *SOM-IRES-Cre::Rosa26-LSL-Cas9, PV-IRES-Cre::Rosa26-LSL-Cas9* or *Emx1-Cre::Rosa26-LSL-Cas9* mice were injected

AAV1-U6-sgRNA^{Npas4} at 250 µm and 500 µm depth (250 nl /site) from pia. Control groups were injected with AAV1-U6-sgRNALacZ.

NRAM labeling: *WT* or *SOM-cre::Ai14* mice were placed under DOX liquid diet 24 hours prior to surgery. DOX liquid contained 2mg/mL of DOX and 5% sucrose, which was placed in tinted bottles to limit light exposure (65). M1 of *SOM-Cre::AI14* mice were injected with pAAV-N-RAM-d2tTA-sEF1a-EGFP; WT were injected with either pAAV-NRAM-d2tTA-TRE-mKate2 or pAAV-N-RAM-d2tTA-sEF1a-EGFP. Viruses were obtained from Dr. Lin's lab (45). Viruses were injected at 250 µm and 500 µm depth (250 nl at each site) from pia.

Perfusions and Slicing

Animals were injected intraperitoneally with 300µl of 10% ketamine and 1% xylazine in saline, 1 hour post training. Once mice were fully anaesthetized and unresponsive, the thoracic cavity was exposed and 5mL of 1% PBS followed by 20 mL of 4% PFA were pumped throughout the circulatory system. Extracted brains were incubated in 4% PFA overnight at 4°C, brains were incubated in 30% Sucrose PBS for cryoprotection at 4°C, until they sink. Subsequently, they were cryosectioned using a Leica CM1950 cryostat (microtome) at a thickness of 35 µm per slice and tissues were stored in PBS with 0.1% sodium azide at 4°C. Slices underwent immunostaining (see details below) and/or stored up to 6 months.

Immunostaining

Brain Allen Atlas were used to collect the sections around the Bregma. Slices were washed 3x in PBS and another 3x in PBS-T (PBS with 1% Triton X-100; 10mins/ wash) for permeabilization. Slices were then incubated in blocking solution (PBS-T with 10% Normal Donkey Serum) for 2 hours at room temperature, and transferred in primary antibody solution to be incubated overnight at 4°C. The primary antibodies utilized was rabbit anti-Npas4 (1:500, Activity Signaling, AS-AB18A-100). The next day, brains were washed 3x10 min in PBS-T, then incubated in corresponding secondary antibodies at room temperature for 2h. The following secondary antibodies were used depending on the experiments: Alexa Fluor® Plus 488 goat anti-rabbit (1:500, Thermo Fisher, A32731), Alexa Fluor® Plus 594 donkey anti-rabbit (1:500, Invitrogen, 1890862) or CyTM5 donkey anti-rabbit (1:500). After incubation, slices were washed 3x10 min in PB and mounted onto microscope slides with VECTASHIELD HardSet Mounting Medium with DAPI (VECTOR Laboratories, H-1200-10). All incubations were processed on a rocking shaker.

Zeiss AxioObserver D1 Inverted Microscope was used to image the brain slices. The primary motor cortex was identified as 100um lateral from the midline. Analyzed images had the objective magnification of 20x, with 25-30% brightness; dimensions of 350 um (width) x 700 um (depth; from pia to Layer 5b). Different exposure times were applied for each channel; BFP (DAPI) was 80ms, phYFP, or Infrared (Npas4) was 8000ms, and RFP (NRAM-mKate2) was 8000ms.

For immunofluorescent studies, 3 brain slices, 315 um apart, were imaged, analyzed, and averaged for each sample. For NRAM studies, to account for the uneven

virus spread and infection across the cortex, 2 brain slices (140um apart) with the most NRAM$^+$ cells were analyzed per brain. Using ImageJ or FIJI software, cells were counted manually and marked to prevent double counts. Counted cells were colocalized with DAPI. Cell density (cells/mm^2) was calculated as: (cell count/ 245000) * 1 000 000. For figures with layer distribution, cells were counted every 30um from pia (0um) to L5b (720 um). For colocalization experiments, each pseudo-colored channel was separately counted and marked prior to merging the channels and counting for colocalizations. Averaged colocalization figures were calculated as: Number of Npas4$^+$ tdTomato$^+$ cells/ Total tdTomato$^+$ (SOM, PV, or EMX) cells and averaged across all samples for each experimental condition. Other calculations in the NRAM studies are described in respective figures above. Cell counting and analyses were conducted blind.

Statistics

For immunofluorescent data, one-tailed bootstrap analyses were conducted. For figures with multiple comparisons, bootstrap analyses with Bonferroni correction were conducted. In bootstrap, each data set were resampled 1000 times to create a distribution, the difference between the two groups were calculated to determine significance. For behavioural analyses, one-way ANOVA was conducted; to compare behaviour across different groups, two-way ANOVA was performed. Statistical analyses for each figure were mentioned in the figure legends.

6. FIGURES

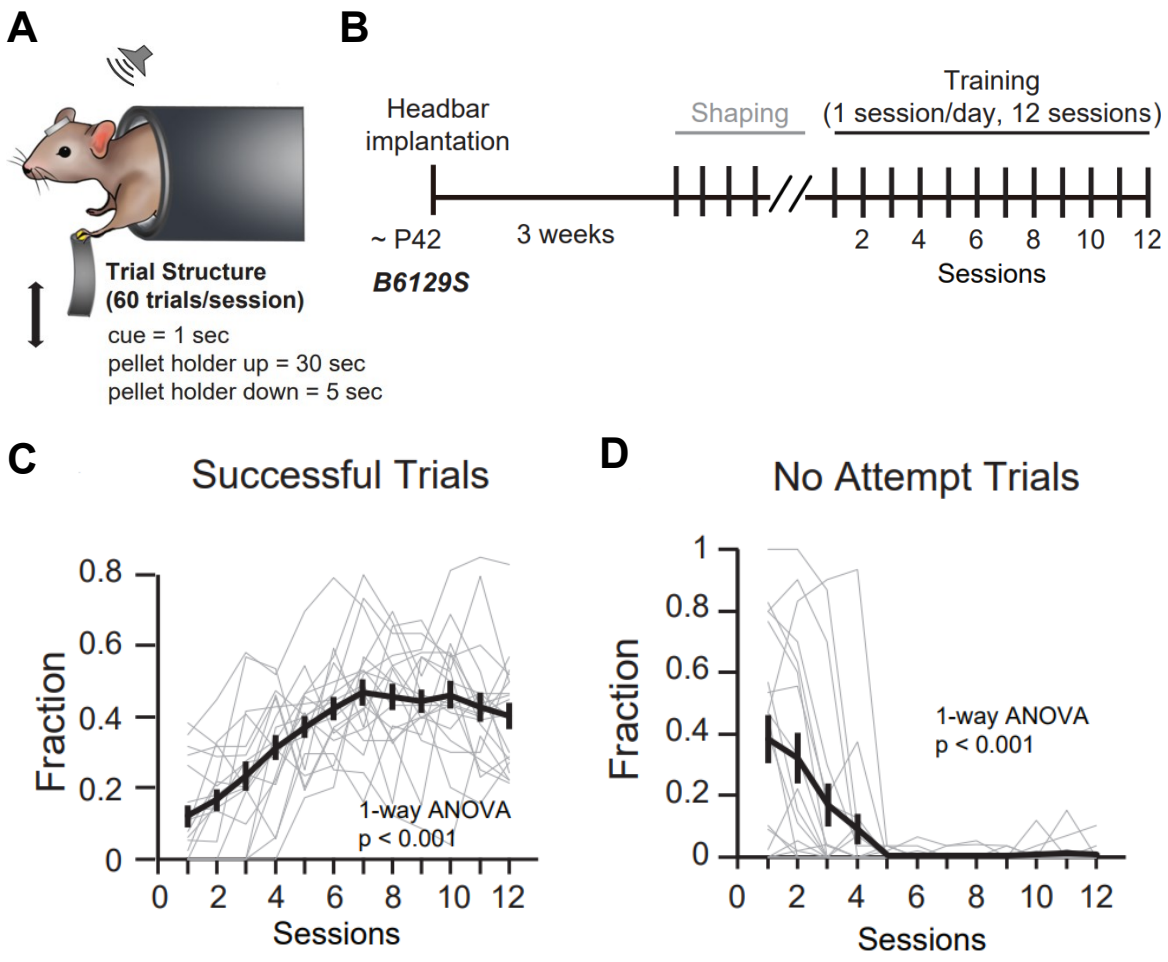

Figure 1: Establishing an Automated Head-fixed Pellet Reaching Task as a Motor Learning Paradigm

A. Schematics of head-fixed pellet reaching paradigm.
B. Experimental timeline
C. Succesful trials in head-fixed pellet reaching task gradually increased and plateaud over 12 sessions. N = 12; one-way ANOVA
D. Mice learned to reach and grasp the pellet and 'no attempt' trials quickly decreased. N = 12, one-way ANOVA

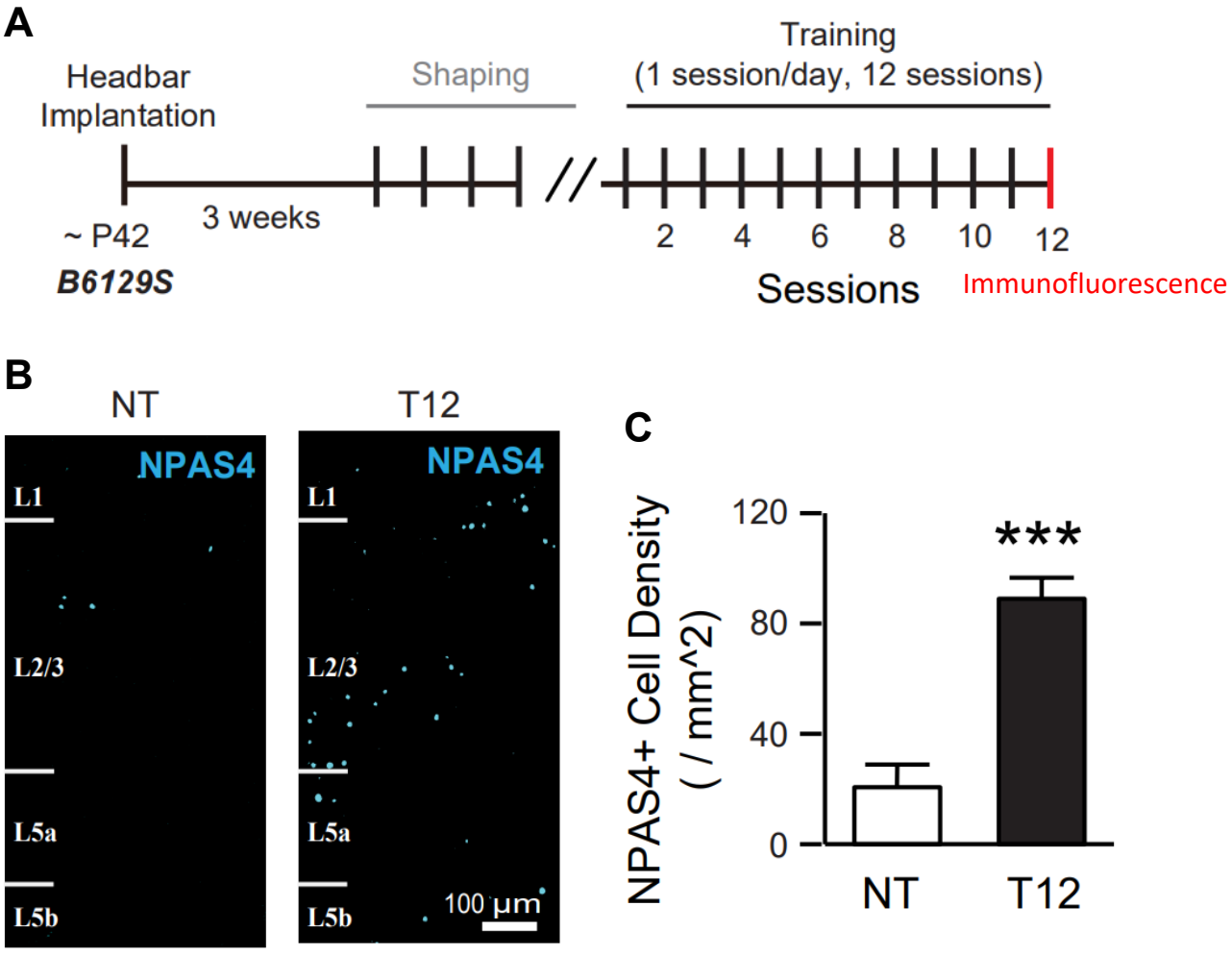

Figure 2: Motor Learning Increased NPAS4 Expression in M1

A. Experimental timeline.
B. Contralateral M1 were immunofluorescently stained for NPAS4 in NT and T12 mice.
C. Motor learning increased NPAS4^{+} cell density in M1. NT: n = 6; T12: n = 7 mice; One-tailed bootstrap test.

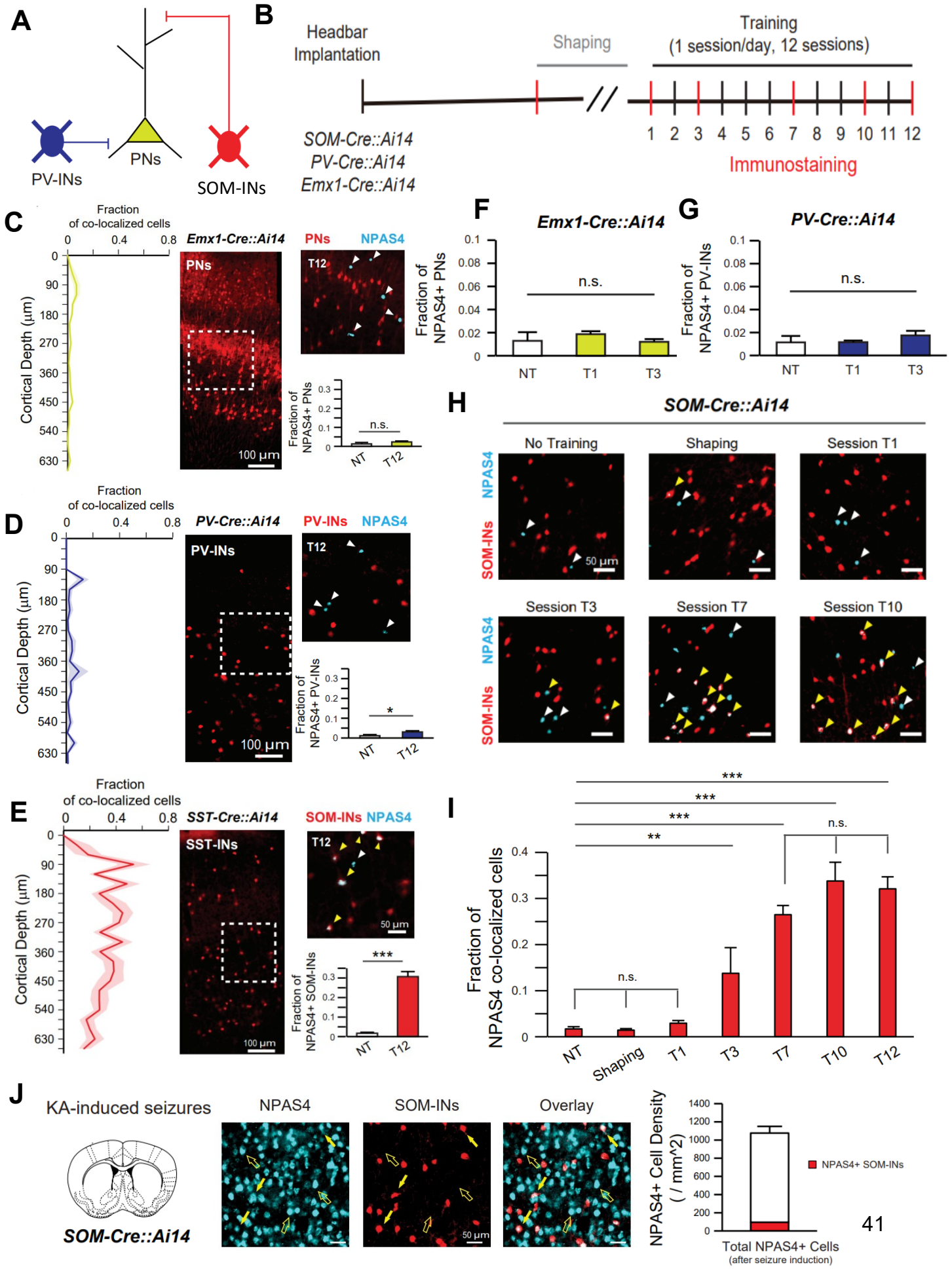
A
PV-INs
PNs
SOM-INs
B
Headbar Implantation
Shaping
Training (1 session/day, 12 sessions)
1 2 3 4 5 6 7 8 9 10 11 12
Immunostaining
SOM-Cre::Ai14
PV-Cre::Ai14
Emx1-Cre::Ai14
C
Fraction of co-localized cells
Emx1-Cre::Ai14
PNs NPAS4
Cortical Depth (µm)
PNs
T12
100 µm
Fraction of NPAS4+ PNs
n.s.
NT T12
D
Fraction of co-localized cells
PV-Cre::Ai14
PV-INs NPAS4
Cortical Depth (µm)
PV-INs
T12
100 µm
Fraction of NPAS4+ PV-INs
*
NT T12
E
Fraction of co-localized cells
SST-Cre::Ai14
SOM-INs NPAS4
Cortical Depth (µm)
SST-INs
T12
50 µm
100 µm
Fraction of NPAS4+ SOM-INs
***
NT T12
F
Emx1-Cre::Ai14
Fraction of NPAS4+ PNs
n.s.
NT T1 T3
G
PV-Cre::Ai14
Fraction of NPAS4+ PV-INs
n.s.
NT T1 T3
H
SOM-Cre::Ai14
No Training
Shaping
Session T1
Session T3
Session T7
Session T10
NPAS4
SOM-INs
50 µm
I
Fraction of NPAS4 co-localized cells
***
***
***
**
n.s.
n.s.
NT Shaping T1 T3 T7 T10 T12
J
KA-induced seizures
SOM-Cre::Ai14
NPAS4
SOM-INs
Overlay
50 µm
NPAS4+ Cell Density (/ mm^2)
NPAS4+ SOM-INs
Total NPAS4+ Cells
(after seizure induction)

Figure 3: NPAS4 is Selectively Expressed within SOM-INs during Motor Learning

A. Schematics of local neural circuitry in M1. PNs (yellow), dendrite-targetting SOM-INs (red), and soma-targeting PV-INs (blue).
B. Experimental timeline and mouse lines used.
C. Left: Mean distribution of low NPAS4$^+$ cells among PNs across the M1 layers at T12. Middle and top right: representative images of trangenically labelled PNs and immuno- staining of NPAS4 in M1. Bottom right: No observable change in NPAS4$^+$ PNs. NT: n = 5; T12: n = 7 mice; Bootstrap analysis
D. Left: Mean distribution of low NPAS4$^+$ cells among PV-INs across the M1 layers at T12. Middle and top right: representative images of trangenically labelled PV-INs and immuno- staining of NPAS4 in M1. Bottom right: Minimal increase of NPAS4$^+$ PV-INs. NT: n = 6; T12: n = 7 mice; Bootstrap analysis
E. Left: Mean distribution of NPAS4$^+$ cells among SOM-INs across the M1 layers at T12. Middle and top right: representative images of trangenically labelled SOM-INs and immuno- staining of NPAS4 in M1. Bottom right: Motor learning-induced increase of NPAS4 expression among SOM-INs. NT: n = 6; T12: n = 10 mice; Bootstrap analysis
F. NPAS4$^+$ PNs at early phases of motor learning relative to baseline. T1: n = 4; T3: n = 7; Bootstrap analysis.
G. NPAS4$^+$ PV-INs at early phases of motor learning relative to baseline. T1: n = 4; T3: n = 7; Bootstrap analysis.
H. Representative images of trangenically-labelled SOM-INs and immunostaining of NPAS4 in M1 at different stages of training. White triangle: NPAS4 only, yellow triangle: NPAS4$^+$ SOM-INs
I. Mean percentage of NPAS4$^+$ SOM-INs gradual increase and plateau (NT: n = 6; Shaping: n = 8; T1: n = 7; T3: n = 8; T7: n = 8; T10: n = 4; T12: n = 10 mice; One-tailed bootstrap test with Bonferroni correction).
J. Right: Schematic seizure induction and mouseline used. Middle: Representative images of trangenic labelling of SOM-INs, immunostaining of NPAS4. Left: Seizure induced maximal NPAS4 expression in M1, across all cell types.

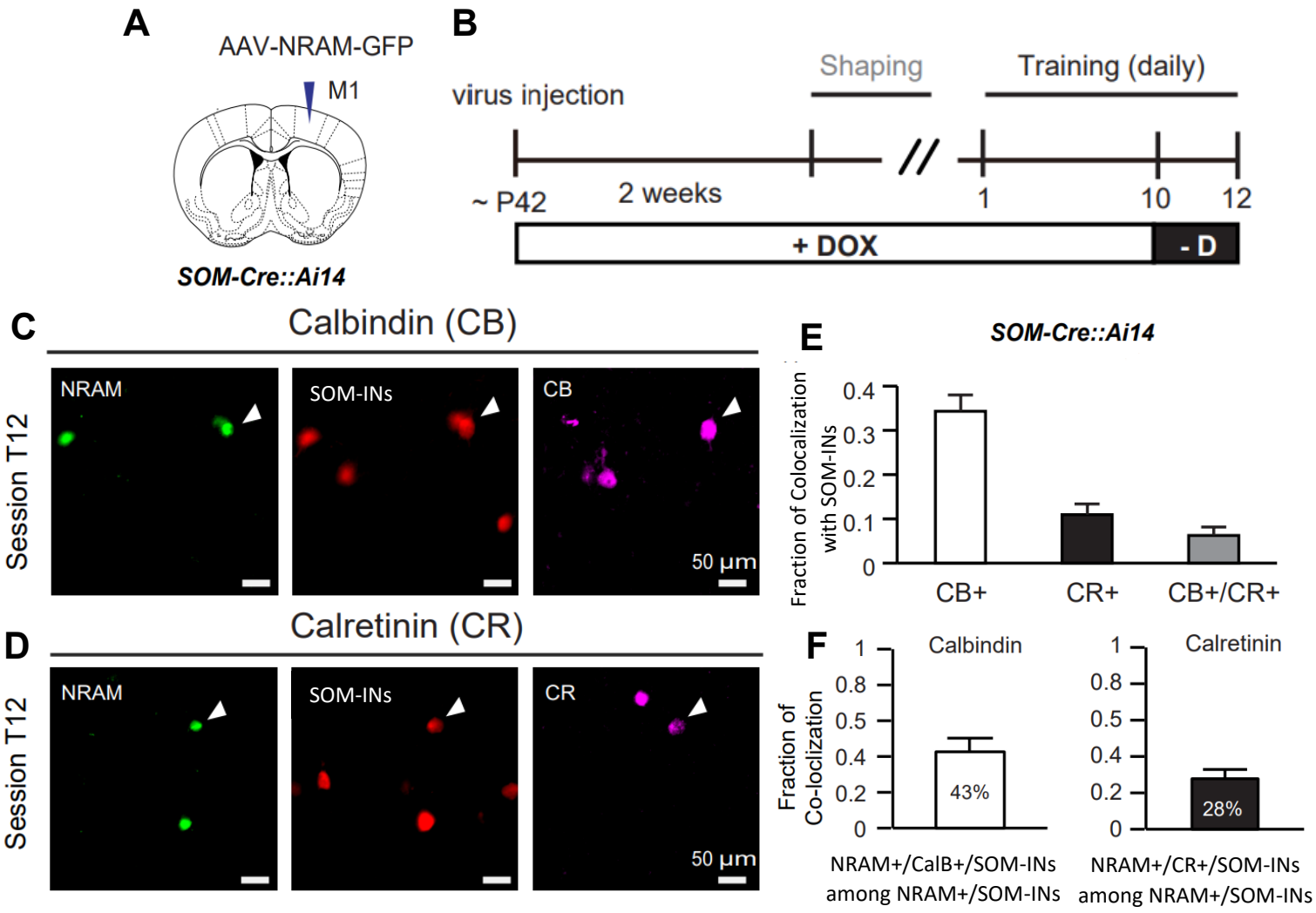

Figure 4: Majority of NPAS4+ SOM-INs during Head-fixed Pellet Reaching Task are Martinotti SOM-INs

A. Schematic of virus injected and mouse lines used to label NPAS4^{+} cells *in vivo* at T12
B. Experimental timeline
C. Representatitve images of NRAM GFP labelling, SOM tdTomato, and infrared CalB immunostaining. White arrow = colocalization of the 3 fluorophores.
D. Representatitve image of NRAM GFP labelling, SOM tdTomato, and infrared CR immunostaining. White arrow = colocalization of the 3 fluorophores.
E. Fraction of SOM-INs in M1 that are CB+ and/or CR+ (Martinotti SOM-INs). N=4
F. Fraction of NPAS4^{+} SOM-INs at T12 that are CB+ and/or CR+ (Martinotti SOM-INs). Calb: n =4; CR: n = 4.

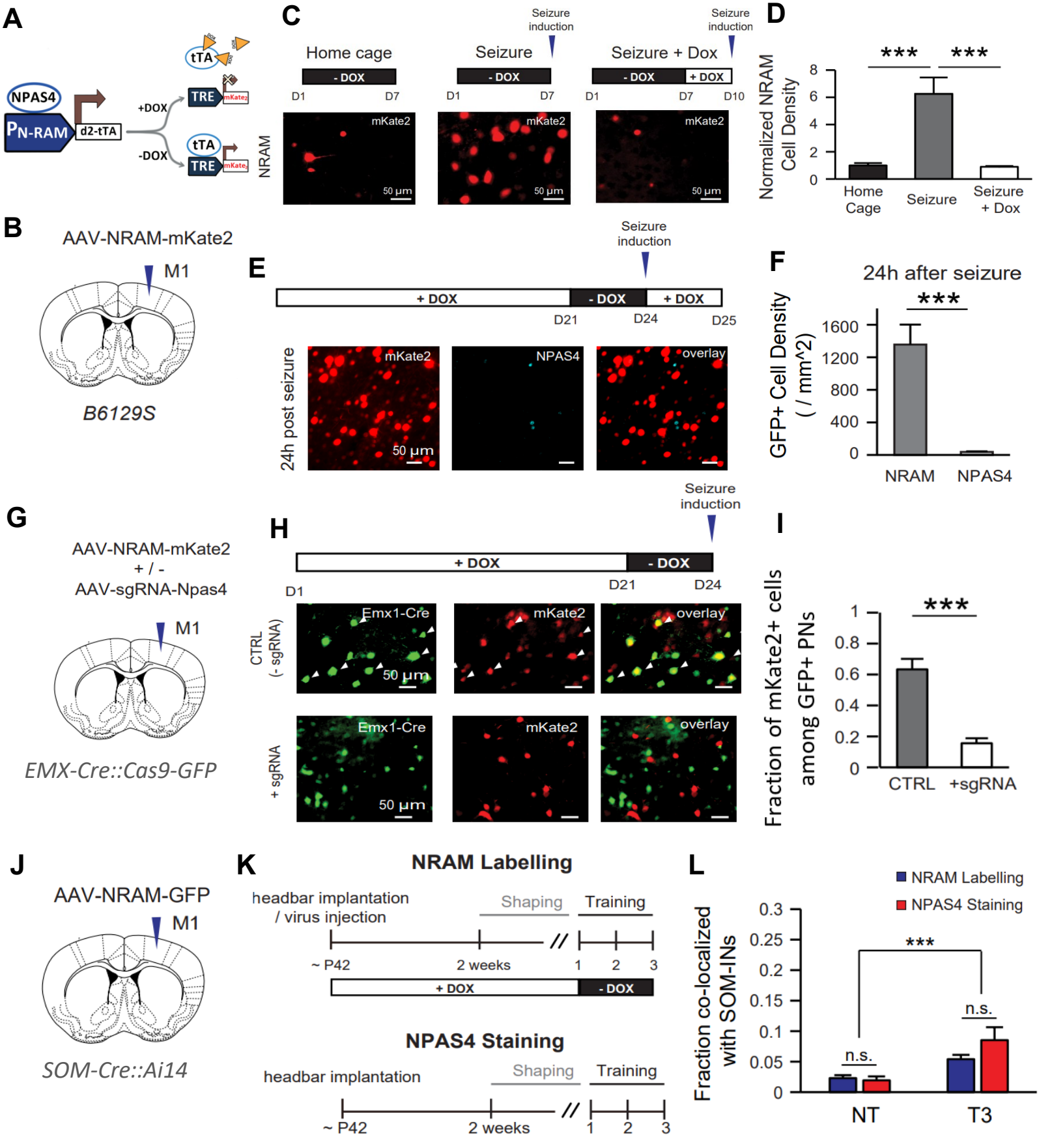
A
NPAS4
PN-RAM
d2-tTA
+DOX
-DOX
tTA
TRE
mKate2
B
AAV-NRAM-mKate2
M1
B6129S
C
Home cage
Seizure
Seizure + Dox
Seizure induction
- DOX
+ DOX
D1
D7
D10
NRAM
mKate2
50 µm
D
Normalized NRAM Cell Density
***
Home Cage
Seizure
Seizure + Dox
E
+ DOX
- DOX
+ DOX
D21
D24
D25
24h post seizure
mKate2
NPAS4
overlay
50 µm
F
24h after seizure
GFP+ Cell Density (/ mm^2)
NRAM
NPAS4
G
AAV-NRAM-mKate2
+ / -
AAV-sgRNA-Npas4
M1
EMX-Cre::Cas9-GFP
H
+ DOX
- DOX
D1
D21
D24
CTRL (- sgRNA)
+ sgRNA
Emx1-Cre
mKate2
overlay
50 µm
I
Fraction of mKate2+ cells among GFP+ PNs
CTRL
+sgRNA
J
AAV-NRAM-GFP
M1
SOM-Cre::Ai14
K
NRAM Labelling
headbar implantation / virus injection
Shaping
Training
~ P42
2 weeks
1
2
3
+ DOX
- DOX
NPAS4 Staining
headbar implantation
L
NRAM Labelling
NPAS4 Staining
Fraction co-localized with SOM-INs
n.s.
NT
T3

Figure 5: Validating the NPAS4-driven Robust Activity Marking (NRAM) System

A. Design of the NPAS4-dependent Robust Activity Marking (NRAM) System. Provided by Dr. Lin's Lab.
B. Schematics of mouseline used and virus injected
C. Top: timeline of DOX liquid diet and seizure induction. Bottom: representative images for each experimetnal cohort
D. Cell density of activity-dependent and DOX-regulated NRAM-labelled cells in home cage, post-seizure, and post-seizure under DOX. Home Cage: n = 3; Seizure: n = 4; Seizure + DOX: n = 3. Bootstrap analysis with Bonferroni correction.
E. Top: DOX is removed 48 hours before behavioural (seizure) induction and 24h before perfusion and NPAS4 immunostaining. Bottom: representative images of NRAM expression and NPAS4 immunostainign 24 hours post-seizure.
F. Cell density of seizure-induced NRAM-labelled cells and NPAS4 expression after 24 hours. N=4; bootstrap analysis.
G. Schematics of mouseline used and virus injected to selectively delete *Npas4* in PNs
H. Top: timeline of DOX liquid diet and seizure induction. Bottom: representative images of NRAM labeling post-seizure induction of *Npas4* PN KO and control mice.
I. Fraction of NPAS4-dependent NRAM-labelled cells among PNs in PN- *Npas4* KO and control mice. PN- *Npas4* KO: n = 4; Control: n = 3. Bootstrap analysis
J. Schematics of mouseline used and virus injected to label NPAS4+ SOM-INs at baseline or at T3 *in vivo*, using NRAM system.
K. Timelines for labelling NPAS4^{+} SOM-INs using NRAM (top) or immunostaining (bottom).
L. Fraction of NPAS4^{+} SOM-INs at baseline and T3 using the NRAM system or immunofluorescent staining. Immunostaining NT: n = 6; NRAM NT: n = 4; Immunostaining T3: n = 7; NRAM T3: n = 8; Bootstrap analysis.

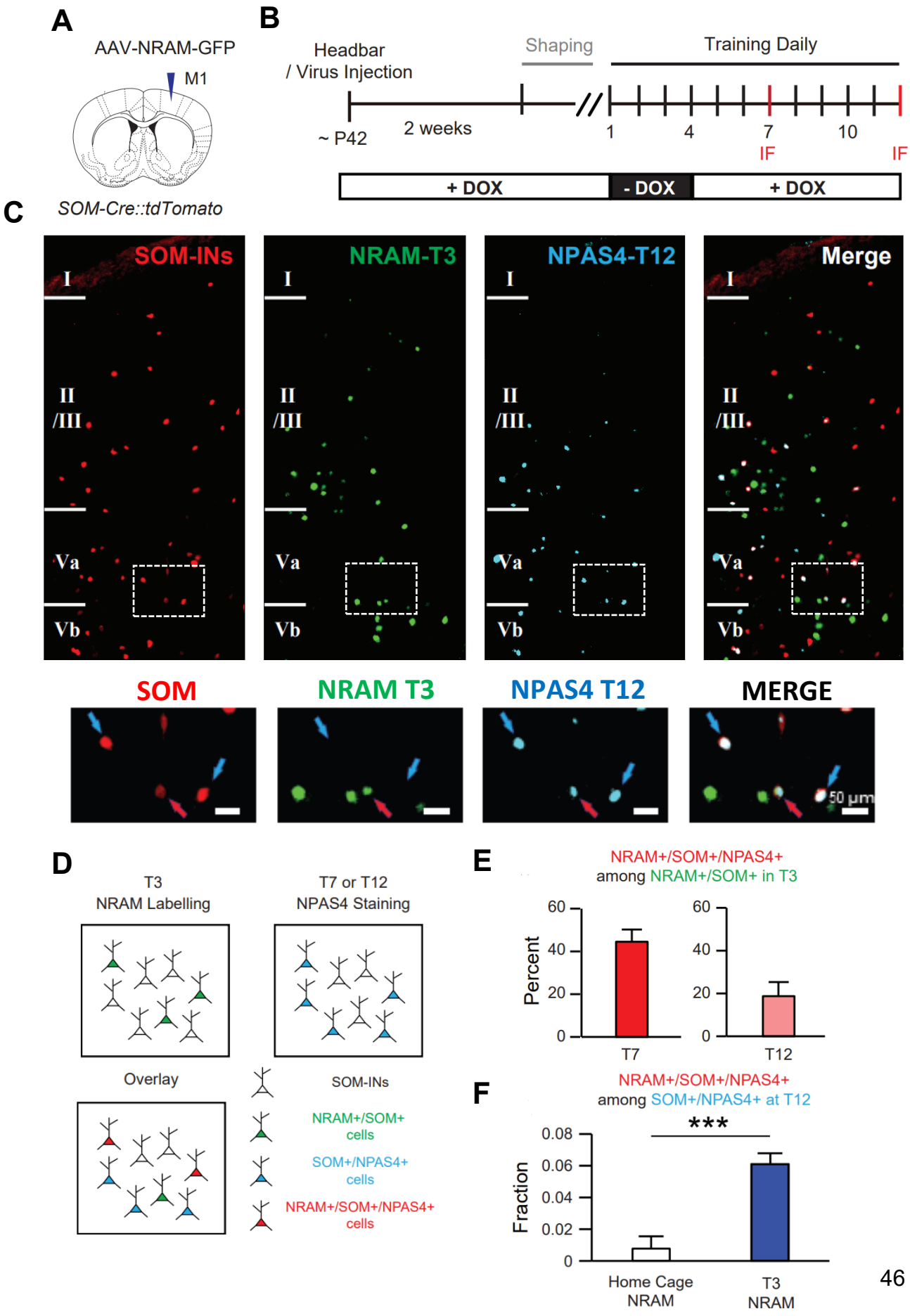
A
AAV-NRAM-GFP
M1
SOM-Cre::tdTomato
B
Headbar
/ Virus Injection
Shaping
Training Daily
~ P42
2 weeks
1
4
7
10
IF
IF
+ DOX
- DOX
+ DOX
C
SOM-INs
NRAM-T3
NPAS4-T12
Merge
I
II
/III
Va
Vb
SOM
NRAM T3
NPAS4 T12
MERGE
50 µm
D
T3
NRAM Labelling
T7 or T12
NPAS4 Staining
Overlay
SOM-INs
NRAM+/SOM+
cells
SOM+/NPAS4+
cells
NRAM+/SOM+/NPAS4+
cells
E
NRAM+/SOM+/NPAS4+
among NRAM+/SOM+ in T3
Percent
60
40
20
0
T7
T12
F
NRAM+/SOM+/NPAS4+
among SOM+/NPAS4+ at T12
***
Fraction
0.08
0.06
0.04
0.02
0
Home Cage
NRAM
T3
NRAM

Figure 6: NPAS4 is Persistently Expressed in an Ensemble of SOM-INs from Early to Late Phases of Learning

A. Schematics of mouse line and virus injected
B. Experimental timeline to label NPAS4^{+} SOM-INs at 2 separate time points
C. Representative image transgenically labelled SOM-INs, NRAM T3 labeling, and NPAS4 T12 immunostaining. Bottom: Zoomed-in version. Cyan arrow = NPAS4^{+} SOM-INs at T12; red arrow = NPAS4-re-expressing SOM-INs
D. Schematic illustration to identify and visualize NPAS4 re-expression within SOM-INs at different stages of motor learning
E. Mean percentages of T3 NRAM+ SOM-INs that continuously expressed NPAS4 at T7 (left, n = 3 mice) or T12 (right, n = 4 mice). Bootstrap analysis
F. Mean percentage of non-task related (home cage) and task-related (T3) NRAM labelled cells that were co-localized with learning-induced NPAS4 at T12. Home cage: n = 3; T3: n = 4 mice, One-tailed bootstrap test.

7. SUPPLEMENTARY FIGURES

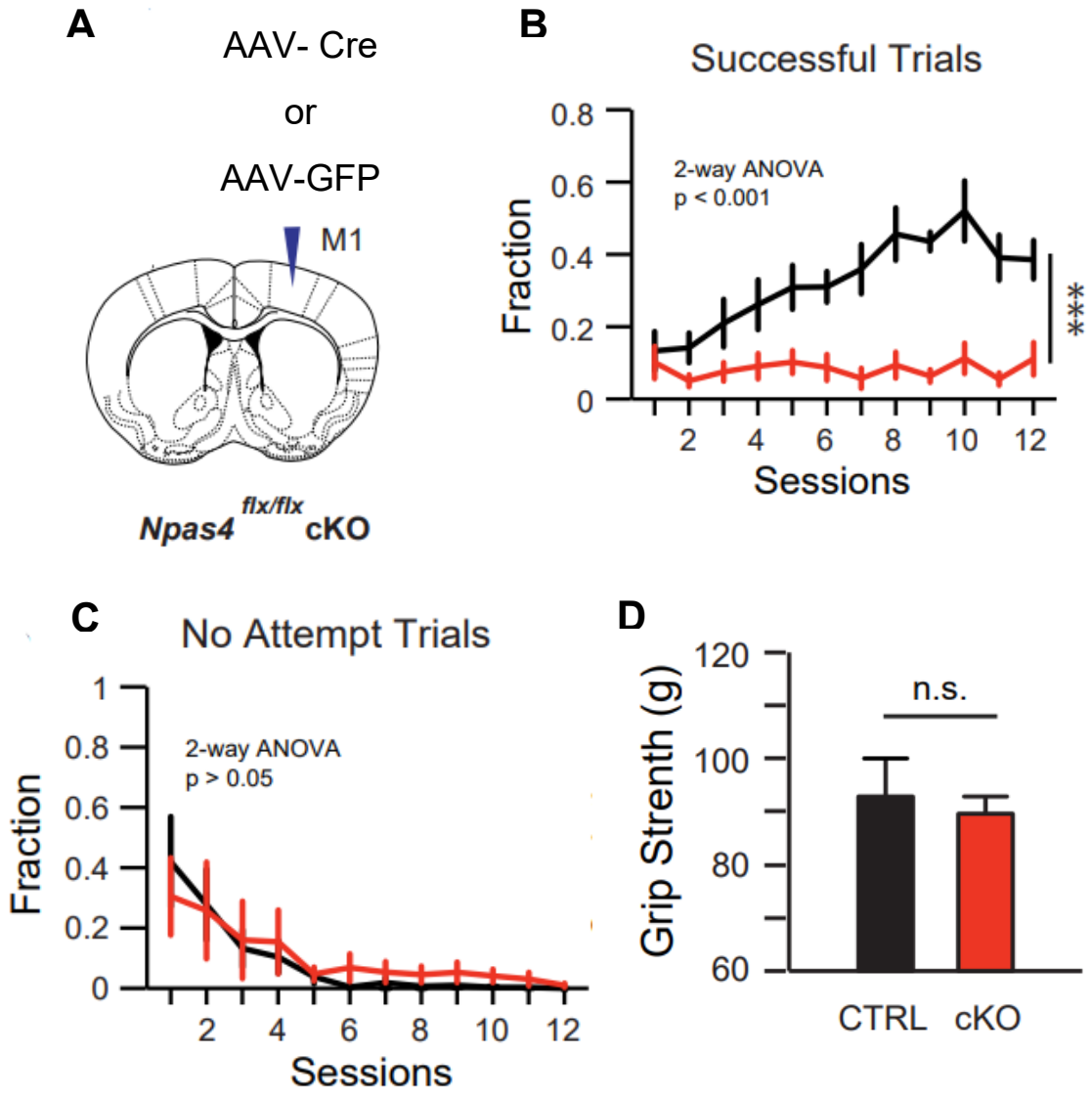

Supplementary Figure 1: Regional *Npas4* in M1 Knock Out Impaired Motor Learning

A. Schematic of virus injected and mouse line used.
B. Mean success rate of *Npas4* cKO mice did not did not improve unlike control mice. CTRL: n = 6; cKO: n = 7 mice; Two-way ANOVA
C. Similar attempt rates between Npas4 cKO and control mice. CTRL: n = 6; cKO: n = 7 mice; Two-way ANOVA
D. Similar mean grip strength between Npas4 cKO and control mice. CTRL: n = 6; cKO: n = 7 mice; One-tailed bootstrap test

Work Conducted by: Dr. Jungwoo Yang

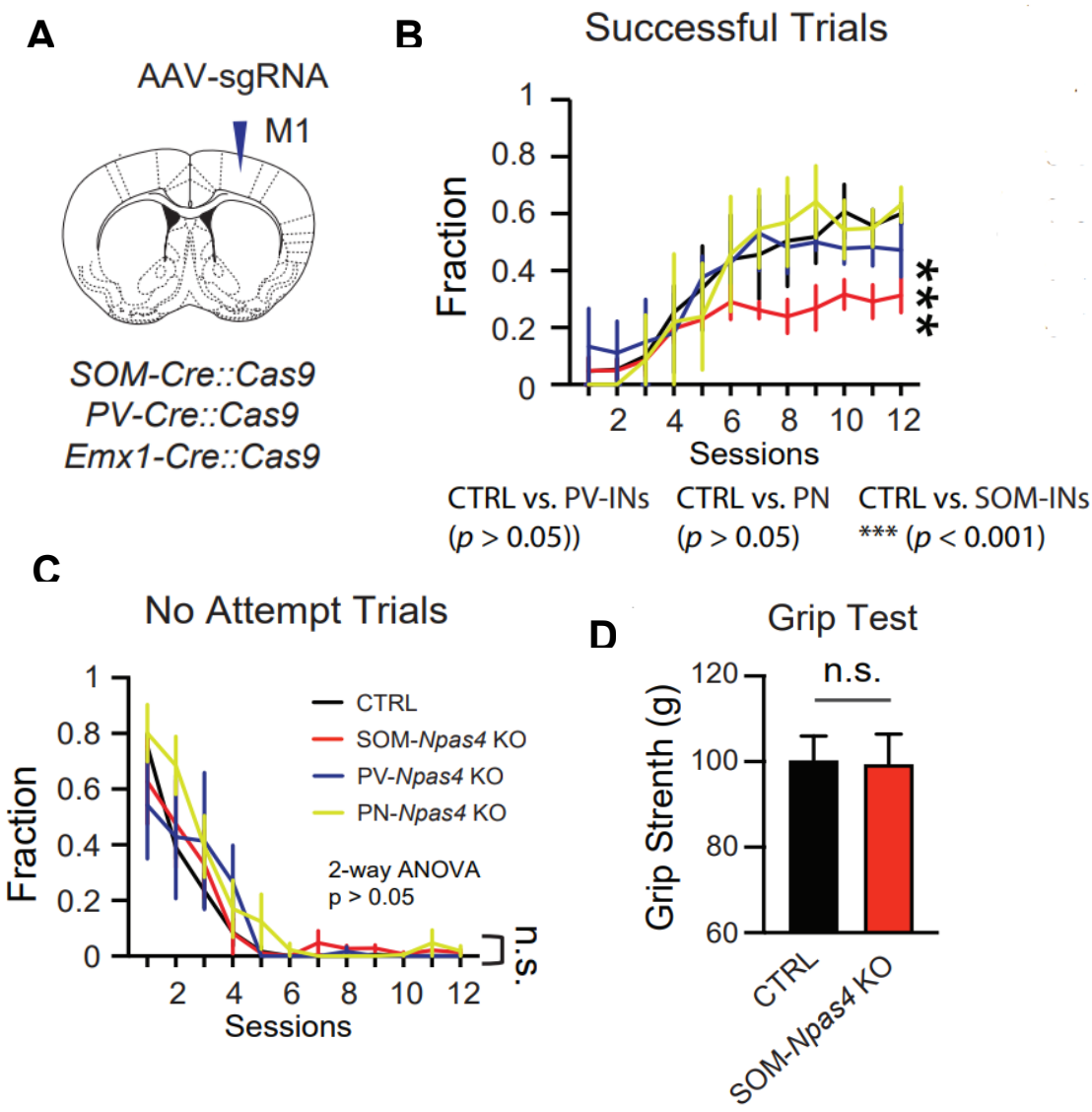

Supplementary Figure 2: Regional and Cell-type Specific Knock Out of Npas4 within SOM-INs of M1 Impaired Motor Learning

A. Schematic of virus injected and mouse lines used.
B. Mean success rate of *Npas4* SOM KO mice was significantly lower compared to *Npas4* PN KO, *Npas4* PV-IN KO and control mice. CTRL: n = 6; SOM: n = 6; PV: n = 5; PN: n = 5 mice; Two-way ANOVA with Tukey's test.
C. Similar attempt rates across all groups. CTRL: n = 6; SOM: n = 6; PV: n = 5; PN: n = 5 mice; Two-way ANOVA with Tukey's test.
D. Similar mean grip strength between *Npas4* SOM KO mice and control mice. One-tailed bootstrap test

Work Conducted by: Dr. Jungwoo Yang

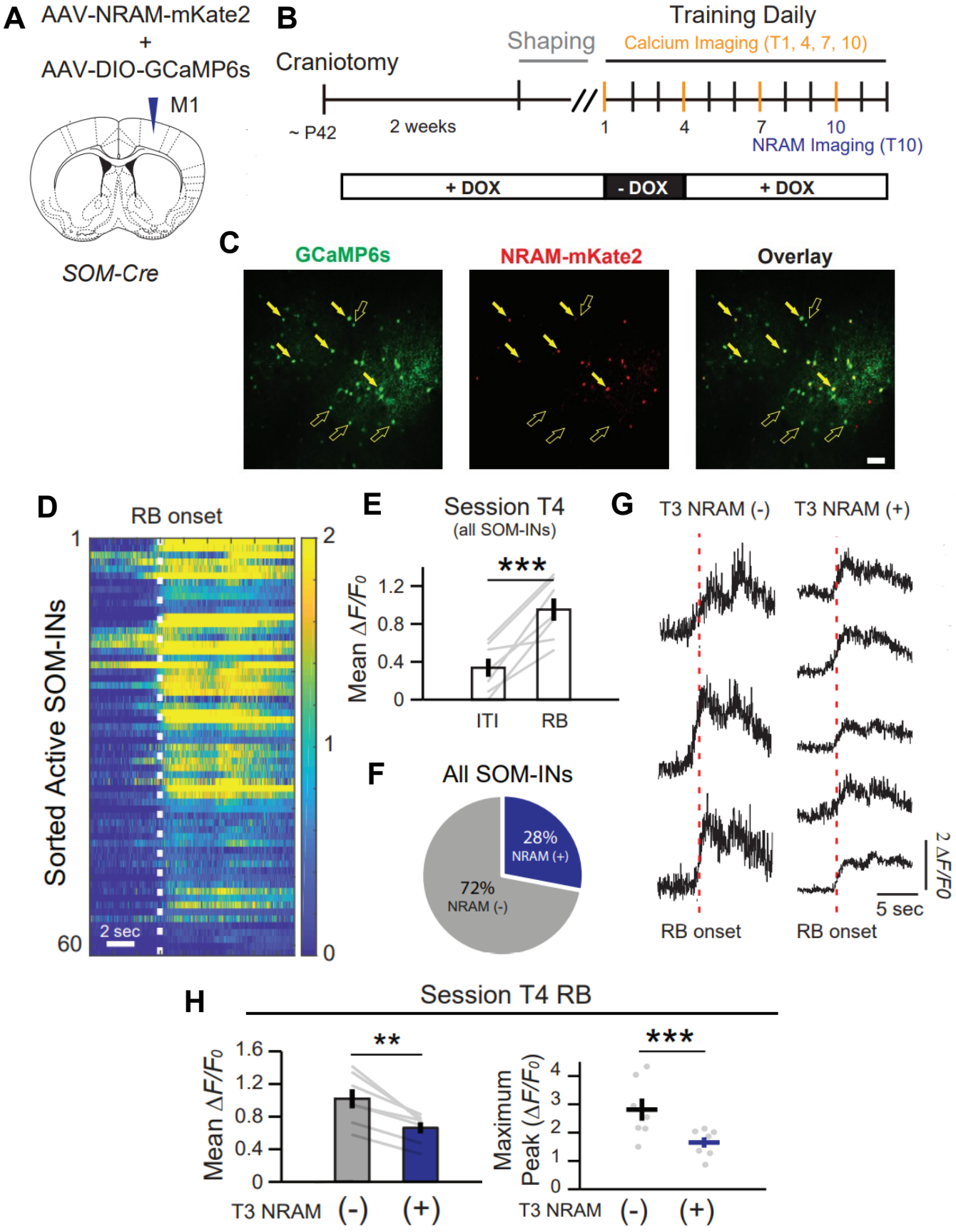
A
AAV-NRAM-mKate2
+
AAV-DIO-GCaMP6s
M1
SOM-Cre
B
Craniotomy
Shaping
Training Daily
Calcium Imaging (T1, 4, 7, 10)
~ P42
2 weeks
1
4
7
10
NRAM Imaging (T10)
+ DOX
- DOX
+ DOX
C
GCaMP6s
NRAM-mKate2
Overlay
D
RB onset
Sorted Active SOM-INs
1
60
2 sec
2
1
0
E
Session T4
(all SOM-INs)
***
Mean ΔF/F0
1.2
0.8
0.4
0
ITI
RB
F
All SOM-INs
28%
NRAM (+)
72%
NRAM (-)
G
T3 NRAM (-)
T3 NRAM (+)
2 ΔF/F0
5 sec
RB onset
RB onset
H
Session T4 RB
**
Mean ΔF/F0
1.6
1.2
0.8
0.4
0
T3 NRAM (-) (+)
***
Maximum Peak (ΔF/F0)
4
3
2
1
0
T3 NRAM (-) (+)

Supplementary Figure 3: A Fraction of NPAS4+ SOM-INs continued to show reduced activity

A. Left, schematic of the virus injected and the mouse line used to track SOM-IN activity and label NPAS4^{+} cells *in vivo*.
B. Experimental timeline to SOM-IN activity using 2-photon microscopy and label NPAS4+ cells at T3 *in vivo.*
C. Representative images of GCaMP-labelled SOM-INs (left), NRAM+ cells at T3 (middle), Merged (right). Filled arrow = NRAM^{+} SOM-INs; empty arrows = NRAM^{-} SOM-INs. Image taken at T10.
D. Representatrive heat map activity from all the active SOM-INs during a reaching bout (RB) from one mouse at T4. Dotted line indicates RB onset.
E. Significantly higher mean $\Delta F/F_0$ during RB than inter-trial interval (ITI) from all SOM-INs at T4 (n = 7 mice; One-tailed bootstrap test).
F. Mean percentage of T3-labelled NRAM^{-} and NRAM^{+} SOM-INs at T4.
G. Example traces of relative change in fluorescent activity ($\Delta F/F_0$) from T3-labelled NRAM^{-} (left) and NRAM^{+} (right) SOM-INs from one mouse at T4. Dotted lines indicate RB onset.
H. Right: Significantly lower mean $\Delta F/F_0$ of T3-labelled NRAM^{+} SOM-INs compared to NRAM^{-} SOM-INs during RBs at T4 (right). One-tailed bootstrap test. Left: Significantly lower mean maximum peak of Ca^{2+} events during RBs of T3-labelled NRAM^{+} SOM-INs compared to NRAM^{-} SOM-INs at T4. One-tailed bootstrap test.

Work Conducted by: Dr. Xuming Yin

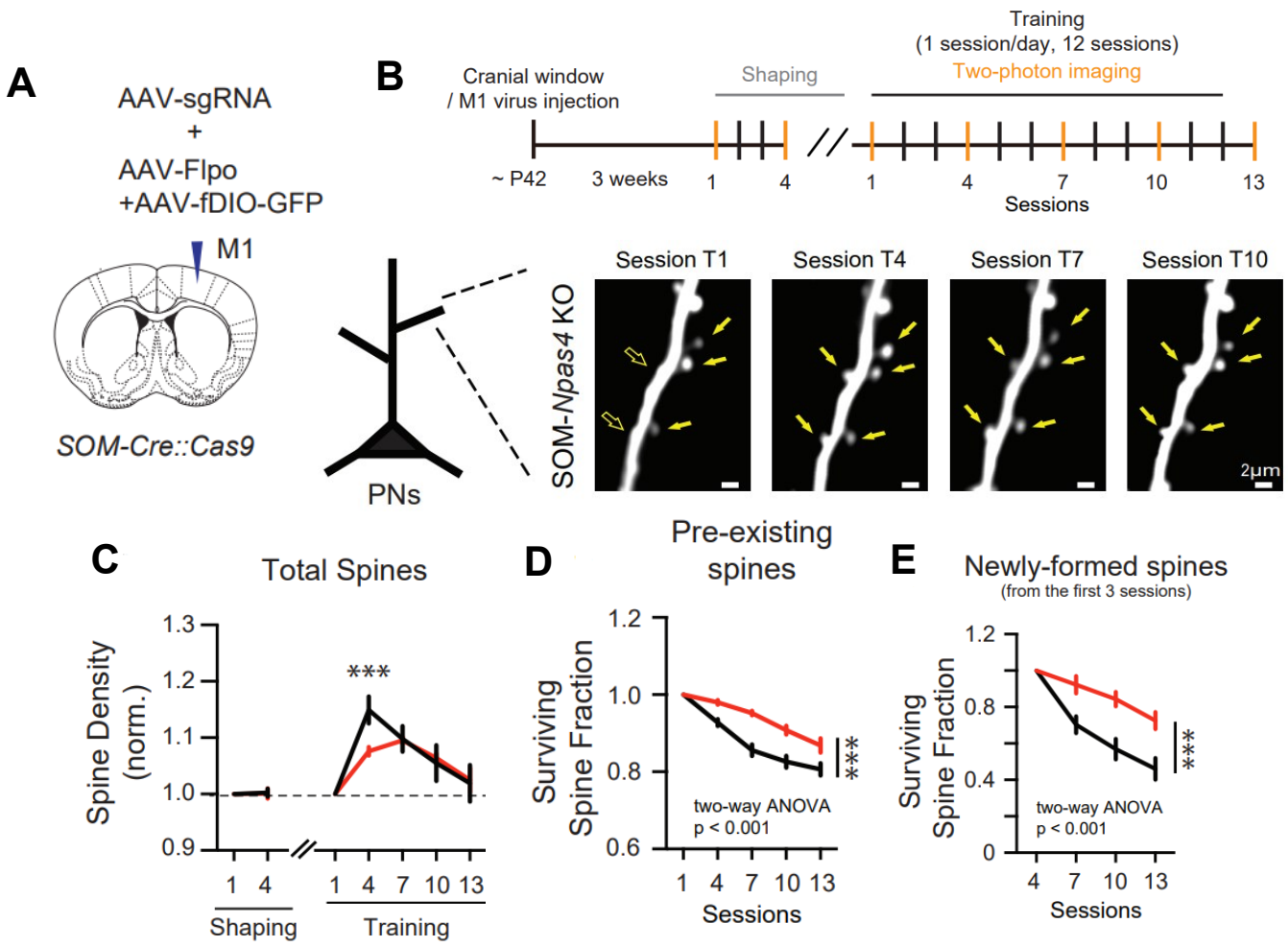

Supplementary Figure 4: Regional and Cell-type Specific *Npas4* Deletion in SOM-INs of M1 Impaired Spine Elimination

A. Schematics of mouse line and virus injected to regionally and selectively knock out *Npas4* in SOM-INs of M1.
B. Top: Experimental timeline of two-photon imaging. Chronic imaging of the same dendritic branch of an L2/3 PN in *Npas4* SOM KO mice. Filled arrows = present spines; open arrows, absent spines. Scale bar = 2μm.
C. Mean spine density of L2/3 PNs in control (shaping, n = 5; training, n = 6 mice) and *Npas4* SOM KO mice, normalized to session 1 of each condition. Shaping: n = 5; Training: n = 6 mice. One-tailed bootstrap test.
D. Significantly higher mean fraction of pre-existing spines that survived across training sessions in *Npas4* SOM KO mice compared to control. Two-way ANOVA
E. Significantly higher mean fraction of newly-formed spines that survived across training sessions in *Npas4* SOM KO mice compared to control. Two-way ANOVA

Work Conducted by: Dr. Jungwoo Yang

8. ACKNOWLEDGEMENT

This project would not have been possible without training, help, and support from my colleagues, friends, and loved ones.

First, I would like to thank my supervisor, Dr. Simon Chen, for 5 years of mentorship and believing in me, even as an undergrad. Most of my research experience and knowledge were cultivated and refined through his training. Secondly, I would like to acknowledge Dr. Jungwoo Yang and Dr. Xuming Yin for training me in various research techniques and collaborating with me to generate a full, in-depth research project. I would also like to thank current and previous lab members. My friends and lab mates, PhD candidates: Candice Lee, Nathaniel Jones, and Nima Raman for their invaluable support and insightful discussions. Our hardware and software engineer, Irina Morozov for constructing and developing the automated head-fixed pellet reaching task. And our lab technician, Liwen Cai, for taking care of the mouse colony and providing artistic drawings for this paper. Lastly, previous lab members, specifically: Tianqi Jiang, Jason Ghossein, and David Ek.

In my personal life, I would like to thank my family who has tirelessly supported and encouraged me throughout my life. My mother who inspires and motivates me to pursue research in medicine and my father who has always been proud of me. My siblings who continuously challenge and drive me to work harder and push harder. My faith in God and my friends who have helped me overcome stress and challenges. Lastly, my partner, Etienne Parent, for the loving and patient support throughout this journey.

REFERENCES

1. Herry, C., & Johansen, J. P. (2014). Encoding of fear learning and memory in distributed neuronal circuits. *Nature neuroscience*, *17*(12), 1644-1654.
2. Reber, P. J. (2008). Cognitive neuroscience of declarative and nondeclarative memory. Advances in psychology, 139, 113-123.
3. Lashley, K. S. in *Society of Experimental Biology Symposium, No. 4: Psychological Mechanisms in Animal Behavior* (eds Danielli, J. F. & Brown, R.) 454–482 (Academic Press, 1950).
4. Josselyn, S. A., Köhler, S., & Frankland, P. W. (2015). Finding the engram. *Nature Reviews Neuroscience*, *16*(9), 521-534.
5. Reijmers, L. G., Perkins, B. L., Matsuo, N., & Mayford, M. (2007). Localization of a stable neural correlate of associative memory. *Science*, *317*(5842), 1230-1233.
6. Han, J. H., Kushner, S. A., Yiu, A. P., Hsiang, H. L., Buch, T., Waisman, A., ... & Josselyn, S. A. (2009). Selective erasure of a fear memory. *Science*, *323*(5920), 1492-1496.
7. Josselyn, S. A. (2010). Continuing the search for the engram: examining the mechanism of fear memories. *Journal of Psychiatry and Neuroscience*, *35*(4), 221-228.
8. Seidenbecher, T., Laxmi, T. R., Stork, O., & Pape, H. C. (2003). Amygdalar and hippocampal theta rhythm synchronization during fear memory retrieval. *Science*, *301*(5634), 846-850.
9. Kim, W. B., & Cho, J. H. (2020). Encoding of contextual fear memory in hippocampal–amygdala circuit. *Nature communications*, *11*(1), 1-22.
10. Liu, X., Ramirez, S., Pang, P. T., Puryear, C. B., Govindarajan, A., Deisseroth, K., & Tonegawa, S. (2012). Optogenetic stimulation of a hippocampal engram activates fear memory recall. *Nature*, *484*(7394), 381-385.
11. Lisman, J. (2017). Criteria for identifying the molecular basis of the engram (CaMKII, PKMzeta). *Molecular brain*, *10*(1), 1-10.
12. Tonegawa, S., Pignatelli, M., Roy, D. S., & Ryan, T. J. (2015). Memory engram storage and retrieval. *Current opinion in neurobiology*, *35*, 101-109.
13. Bliss, T. V., & Lømo, T. (1973). Long-lasting potentiation of synaptic transmission in the dentate area of the anaesthetized rabbit following stimulation of the perforant path. *The Journal of physiology*, *232*(2), 331-356.
14. Josselyn, S. A., & Tonegawa, S. (2020). Memory engrams: Recalling the past and imagining the future. *Science*, 367(6473).
15. Froemke, R. C., Merzenich, M. M., & Schreiner, C. E. (2007). A synaptic memory trace for cortical receptive field plasticity. *Nature*, *450*(7168), 425-429.
16. Barron, H. C., Vogels, T. P., Behrens, T. E., & Ramaswami, M. (2017). Inhibitory engrams in perception and memory. *Proceedings of the National Academy of Sciences*, *114*(26), 6666-6674.
17. Hattori, R., Kuchibhotla, K., Froemke, R. et al. Functions and dysfunctions of neocortical inhibitory neuron subtypes. Nat Neurosci 20, 1199–1208 (2017). https://doi.org/10.1038/nn.4619

18. Wolff, S. B., Gründemann, J., Tovote, P., Krabbe, S., Jacobson, G. A., Müller, C., ... & Lüthi, A. (2014). Amygdala interneuron subtypes control fear learning through disinhibition. Nature, 509(7501), 453-458.
19. Yau, J. O. Y., Chaichim, C., Power, J. M., & McNally, G. P. (2021). The roles of basolateral amygdala parvalbumin neurons in fear learning. Journal of Neuroscience, 41(44), 9223-9234.
20. Stefanelli, T., Bertollini, C., Lüscher, C., Muller, D., & Mendez, P. (2016). Hippocampal somatostatin interneurons control the size of neuronal memory ensembles. Neuron, 89(5), 1074-1085.
21. Giorgi, C., & Marinelli, S. (2021). Roles and Transcriptional Responses of Inhibitory Neurons in Learning and Memory. *Frontiers in Molecular Neuroscience*, 113.
22. Krakauer, J. W., Hadjiosif, A. M., Xu, J., Wong, A. L., & Haith, A. M. (2019). Motor learning. *Compr Physiol*, *9*(2), 613-663.
23. Whishaw, I. Q., Faraji, J., Kuntz, J., Mirza Agha, B., Patel, M., Metz, G. A., & Mohajerani, M. H. (2017). Organization of the reach and grasp in head-fixed vs freely-moving mice provides support for multiple motor channel theory of neocortical organization. *Experimental brain research*, *235*(6), 1919-1932.
24. Asanuma, H., & Pavlides, C. (1997). Neurobiological basis of motor learning in mammals. Neuroreport: An International Journal for the Rapid Communication of Research in Neuroscience.
25. Papale, A. E., & Hooks, B. M. (2018). Circuit changes in motor cortex during motor skill learning. *Neuroscience*, 368, 283-297.
26. Kawai, R., Markman, T., Poddar, R., Ko, R., Fantana, A. L., Dhawale, A. K., ... & Ölveczky, B. P. (2015). Motor cortex is required for learning but not for executing a motor skill. *Neuron*, *86*(3), 800-812.
27. Gremel, C. M., & Costa, R. M. (2013). Premotor cortex is critical for goal-directed actions. Frontiers in computational neuroscience, 7, 110.
28. Hwang, F. J., Roth, R. H., Wu, Y. W., Sun, Y., Kwon, D. K., Liu, Y., & Ding, J. B. (2022). Motor learning selectively strengthens cortical and striatal synapses of motor engram neurons. Neuron.
29. Hikosaka, O., Takikawa, Y., & Kawagoe, R. (2000). Role of the basal ganglia in the control of purposive saccadic eye movements. Physiological reviews, 80(3), 953-978.
30. Asanuma, H. (1981). Functional role of sensory inputs to the motor cortex. Progress in neurobiology, 16(3-4), 241-262.
31. Thach, W. T. (2007, September). Cerebellar inputs to motor cortex. In Ciba Foundation Symposium 132-Motor Areas of the Cerebral Cortex: Motor Areas of The Cerebral Cortex: Ciba Foundation Symposium 132 (pp. 201-230). Chichester, UK: John Wiley & Sons, Ltd..
32. Petrof, I., Viaene, A. N., & Sherman, S. M. (2015). Properties of the primary somatosensory cortex projection to the primary motor cortex in the mouse. Journal of neurophysiology, 113(7), 2400-2407.
33. Peters, A. J., Chen, S. X., & Komiyama, T. (2014). Emergence of reproducible spatiotemporal activity during motor learning. *Nature*, *510*(7504), 263-267.

34. Chen, S. X., Kim, A. N., Peters, A. J., & Komiyama, T. (2015). Subtype-specific plasticity of inhibitory circuits in motor cortex during motor learning. *Nature neuroscience*, *18*(8), 1109-1115.
35. Adler, A., Zhao, R., Shin, M. E., Yasuda, R., & Gan, W. B. (2019). Somatostatin-expressing interneurons enable and maintain learning-dependent sequential activation of pyramidal neurons. *Neuron*, *102*(1), 202-216.
36. West, A. E., Griffith, E. C., & Greenberg, M. E. (2002). Regulation of transcription factors by neuronal activity. *Nature Reviews Neuroscience*, *3*(12), 921-931.
37. Flavell, S. W., & Greenberg, M. E. (2008). Signaling mechanisms linking neuronal activity to gene expression and plasticity of the nervous system. Annual review of neuroscience, 31, 563.
38. Lin, Y., Bloodgood, B. L., Hauser, J. L., Lapan, A. D., Koon, A. C., Kim, T. K., ... & Greenberg, M. E. (2008). Activity-dependent regulation of inhibitory synapse development by Npas4. *Nature*, *455*(7217), 1198-1204.
39. Bloodgood, B. L., Sharma, N., Browne, H. A., Trepman, A. Z., & Greenberg, M. E. (2013). The activity-dependent transcription factor NPAS4 regulates domain-specific inhibition. *Nature*, *503*(7474), 121-125.
40. Ramamoorthi, K., Fropf, R., Belfort, G. M., Fitzmaurice, H. L., McKinney, R. M., Neve, R. L., ... & Lin, Y. (2011). Npas4 regulates a transcriptional program in CA3 required for contextual memory formation. *Science*, *334*(6063), 1669-1675.
41. Brigidi, G. S., Hayes, M. G., Santos, N. P. D., Hartzell, A. L., Texari, L., Lin, P. A., ... & Bloodgood, B. L. (2019). Genomic decoding of neuronal depolarization by stimulus-specific NPAS4 heterodimers. *Cell*, *179*(2), 373-391.
42. Spiegel, I., Mardinly, A. R., Gabel, H. W., Bazinet, J. E., Couch, C. H., Tzeng, C. P., ... & Greenberg, M. E. (2014). Npas4 regulates excitatory-inhibitory balance within neural circuits through cell-type-specific gene programs. *Cell*, *157*(5), 1216-1229.
43. Sun, X., & Lin, Y. (2016). Npas4: linking neuronal activity to memory. *Trends in neurosciences*, *39*(4), 264-275.
44. Latchman, D. S. (1997). Transcription factors: an overview. *The international journal of biochemistry & cell biology*, *29*(12), 1305-1312.
45. Sun, X., Bernstein, M. J., Meng, M., Rao, S., Sørensen, A. T., Yao, L., ... & Lin, Y. (2020). Functionally distinct neuronal ensembles within the memory engram. *Cell*, *181*(2), 410-423.
46. Sørensen, A. T., Cooper, Y. A., Baratta, M. V., Weng, F. J., Zhang, Y., Ramamoorthi, K., ... & Lin, Y. (2016). A robust activity marking system for exploring active neuronal ensembles. *Elife*, *5*, e13918.
47. Weng, F. J., Garcia, R. I., Lutzu, S., Alviña, K., Zhang, Y., Dushko, M., ... & Lin, Y. (2018). Npas4 is a critical regulator of learning-induced plasticity at mossy fiber-CA3 synapses during contextual memory formation. *Neuron*, *97*(5), 1137-1152.
48. Park, A., Jacob, A. D., Walters, B. J., Park, S., Rashid, A. J., Jung, J. H., ... & Josselyn, S. A. (2020). A time-dependent role for the transcription factor CREB in neuronal allocation to an engram underlying a fear memory revealed using a novel in vivo optogenetic tool to modulate CREB function. *Neuropsychopharmacology*, *45*(6), 916-924.

49. Rao-Ruiz, P., Couey, J. J., Marcelo, I. M., Bouwkamp, C. G., Slump, D. E., Matos, M. R., ... & Kushner, S. A. (2019). Engram-specific transcriptome profiling of contextual memory consolidation. *Nature communications*, *10*(1), 1-14.
50. Guenthner, C. J., Miyamichi, K., Yang, H. H., Heller, H. C., & Luo, L. (2013). Permanent genetic access to transiently active neurons via TRAP: targeted recombination in active populations. Neuron, 78(5), 773-784.
51. Zhao J, Nassar MA, Gavazzi I, Wood JN. Tamoxifen-inducible NaV1.8-CreERT2 recombinase activity in nociceptive neurons of dorsal root ganglia. Genesis. 2006 Aug;44(8):364-71. doi: 10.1002/dvg.20224. PMID: 16850455.
52. Cunha, C., Brambilla, R., & Thomas, K. L. (2010). A simple role for BDNF in learning and memory?. *Frontiers in molecular neuroscience*, *3*, 1.
53. Nigro, M. J., Hashikawa-Yamasaki, Y., & Rudy, B. (2018). Diversity and connectivity of layer 5 somatostatin-expressing interneurons in the mouse barrel cortex. *Journal of Neuroscience*, *38*(7), 1622-1633.
54. Ma, Y., Hu, H., Berrebi, A. S., Mathers, P. H., & Agmon, A. (2006). Distinct subtypes of somatostatin-containing neocortical interneurons revealed in transgenic mice. *Journal of Neuroscience*, *26*(19), 5069-5082.
55. Wang, Y., Toledo-Rodriguez, M., Gupta, A., Wu, C., Silberberg, G., Luo, J., & Markram, H. (2004). Anatomical, physiological and molecular properties of Martinotti cells in the somatosensory cortex of the juvenile rat. *The Journal of physiology*, *561*(1), 65-90.
56. Gidon, A., and Segev, I. (2012). Principles governing the operation of synaptic inhibition in dendrites. *Neuron* 75, 330-341.
57. Hayama, T., Noguchi, J., Watanabe, S., Takahashi, N., Hayashi-Takagi, A., Ellis-Davies, G.C., Matsuzaki, M., and Kasai, H. (2013). GABA promotes the competitive selection of dendritic spines by controlling local Ca2+ signaling. *Nature neuroscience* 16, 1409-1416.
58. Steele, P.M., and Mauk, M.D. (1999). Inhibitory control of LTP and LTD: stability of synapse strength. *Journal of neurophysiology* 81, 1559-1566.
59. Yang, G., Lai, C. S. W., Cichon, J., Ma, L., Li, W., & Gan, W. B. (2014). Sleep promotes branch-specific formation of dendritic spines after learning. *Science*, *344*(6188), 1173-1178.
60. Karnani, M. M., Agetsuma, M., & Yuste, R. (2014). A blanket of inhibition: functional inferences from dense inhibitory connectivity. *Current opinion in Neurobiology*, *26*, 96-102.
61. Obermayer, J., Heistek, T. S., Kerkhofs, A., Goriounova, N. A., Kroon, T., Baayen, J. C., ... & Mansvelder, H. D. (2018). Lateral inhibition by Martinotti interneurons is facilitated by cholinergic inputs in human and mouse neocortex. *Nature communications*, *9*(1), 1-14.
62. Krishnamurthy, P., Silberberg, G., & Lansner, A. (2015). Long-range recruitment of Martinotti cells causes surround suppression and promotes saliency in an attractor network model. *Frontiers in Neural Circuits*, *9*, 60.
63. Taniguchi, M., Carreira, M. B., Cooper, Y. A., Bobadilla, A. C., Heinsbroek, J. A., Koike, N., ... & Cowan, C. W. (2017). HDAC5 and its target gene, Npas4, function in the nucleus accumbens to regulate cocaine-conditioned behaviors. *Neuron*, *96*(1), 130-144.

64. Sharma, N., Pollina, E. A., Nagy, M. A., Yap, E. L., DiBiase, F. A., Hrvatin, S., ... & Greenberg, M. E. (2019). ARNT2 tunes activity-dependent gene expression through NCoR2-mediated repression and NPAS4-mediated activation. *Neuron*, *102*(2), 390-406.
65. Redelsperger, I. M., Taldone, T., Riedel, E. R., Lepherd, M. L., Lipman, N. S., & Wolf, F. R. (2016). Stability of Doxycycline in Feed and Water and Minimal Effective Doses in Tetracycline-Inducible Systems. *Journal of the American Association for Laboratory Animal Science : JAALAS,* 55(4), 467–474.

APPENDIX

Link for Rights, sharing, and embargo policies from Cell Press:

https://www.cell.com/rights-sharing-embargoes#:~:text=Most%20Cell%20Press%20articles%20are,or%20blog%20prior%20to%20publication.

Link for Permission Information from Cell Press:

https://www.cell.com/pb-assets/journals/research/matter/Matter_IfA.PDF

Permissions

If you want to use excerpts or images, original or adapted, from articles that you have published in a Cell Press journal, you do not need to ask our permission. Our policy only requires that you cite the original publication.

If you want to use excerpts from copyrighted work in your Cell Press submission, you must obtain written permission from the copyright owners and cite the original publication. For information about how to request permission to use copyrighted material, including work published elsewhere at Elsevier, please visit our permissions page.

If you have adapted a published figure, you may or may not need permission from the copyright owner, depending on how much the adaptation resembles the original. When in doubt, check with the copyright owner and cite the original article.